# THE MECHANISMS OF ATP - BIOMACROMOLECULE INTERACTIONS

A THESIS SUBMITTED TO

THE GRADUATE SCHOOL OF ENGINEERING AND SCIENCE

OF

BILKENT UNIVERSITY

IN PARTIAL FULFILLMENT OF THE REQUIREMENTS FOR THE DEGREE OF

MASTER OF SCIENCE

IN

CHEMISTRY

By

CANSIN AYVAZ

DECEMBER 2023

THE MECHANISMS OF ATP - BIOMACROMOLECULE INTERACTIONS

BY CANSIN AYVAZ

DECEMBER 2023

We certify that we have read this thesis and that in our opinion it is fully adequate, in scope and in quality, as a thesis for the degree of Master of Science.

_____

Halil Ibrahim Okur (Advisor)

_____

Aykut Erbaş

_____

Sreeparna Banerjee

Approved for the Graduate School of Engineering and Science:

_____

Orhan Arıkan

Director of the Graduate School

# ABSTRACT


**THE MECHANISMS OF ATP-BIOMACROMOLECULE INTERACTIONS**

Cansın Ayvaz

M.S. in Chemistry

Advisor: Dr. Halil Ibrahim Okur

December 2023

Adenosine triphosphate (ATP), one of the most important biomolecules of life, plays a vital role as the primary energy source within cells for essential biological functions. It has recently been discovered that ATP can also serve as a biological hydrotrope to destabilize protein aggregates and fibers. This thesis aims to investigate the recently discovered hydrotropic behavior of ATP and its interaction mechanisms with biomacromolecules, particularly poly(*N*-isopropylacrylamide) (PNIPAM), using a multi-experimental approach combined with molecular dynamics (MD) simulations. Adapting the bottom-up approach, the phase behavior of macromolecules is examined through phase transition and ATR-FTIR measurements. Additionally, site-specific interactions are identified with quantitative $^{1}$H-NMR spectroscopic studies, and the hydration shell structure and cluster morphologies of ATP molecules are explored through Multivariate Curve Resolution (MCR) Raman experiments. It is demonstrated that adenine and adenosine subgroups show negligible effect on the solubility of macromolecules, whereas ATP, AMP, and triphosphate exhibited purely salting-out behavior, and induced the aggregation of macromolecules. In stark contrast to the recently discovered hydrotropic behavior of ATP, no specific interactions between the macromolecule and ATP were observed in spectroscopic ATR-FTIR and $^{1}$H-NMR measurements, as well as MD simulations. Surprisingly, at elevated concentrations, self-association of ATP was observed leading to partial

destabilization of larger PNIPAM aggregates to smaller ones. In the absence of ATP binding sites, interactions with random-coil-like structured macromolecules do not lead to effective hydrotropic action of ATP. Instead, they function more as stabilizers rather than solubilizing the macromolecules.

*Keywords:* Adenosine triphosphate, adenosine monophosphate, tripolyphosphate, adenine, adenosine, hydrotropes, thermoresponsive polymers, PNIPAM, PDEA

# ÖZET


## ATP-BİYOMAKROMOLEKÜL ETKİLEŞİMLERİNİN MEKANİZMALARI

Cansın Ayvaz

Kimya | Yüksek Lisans

Danışman: Dr. Halil Ibrahim Okur

Aralık 2023

Yaşamın en önemli biyomoleküllerinden biri olan adenozin trifosfat (ATP), temel biyolojik işlevler için hücrelerde birincil enerji kaynağı olarak hayati bir rol oynar. Son zamanlarda ATP'nin protein agregatlarını ve liflerini dengesizleştirmek için biyolojik bir hidrotrop görevi görebileceği keşfedildi. Bu tez, ATP'nin yakın zamanda keşfedilen hidrotropik davranışını ve bunun biyomakromoleküllerle, özellikle de poli (*N*-izopropilakrilamid) (PNIPAM) ile etkileşim mekanizmalarını, moleküler dinamik (MD) simülasyonlarıyla birleştirilmiş çoklu deneysel bir yaklaşım kullanarak araştırmayı amaçlamaktadır. Aşağıdan yukarıya yaklaşım benimsenerek makromoleküllerin faz davranışı, faz geçişi ve ATR-FTIR ölçümleri yoluyla incelenir. Ek olarak, sahaya özgü etkileşimler niceliksel 1H-NMR spektroskopik çalışmalarla tanımlanır ve ATP moleküllerinin hidrasyon kabuk yapısı ve küme morfolojileri Çok Değişkenli Eğri Çözümleme (MCR) Raman deneyleri aracılığıyla araştırılır. Adenin ve adenozin alt gruplarının makromoleküllerin çözünürlüğü üzerinde ihmal edilebilir bir etkisi olduğu gösterilmiştir, öte yandan ATP, AMP ve trifosfat ise tamamen tuzlanma davranışı sergilemiş ve makromoleküllerin agregasyonuna neden olmuştur. ATP'nin yakın zamanda keşfedilen hidrotropik davranışının tam tersine, spektroskopik ATR-FTIR ve 1H-NMR ölçümlerinin yanı sıra MD simülasyonlarında makromolekül ile ATP arasında hiçbir spesifik etkileşim gözlenmemiştir. Şaşırtıcı bir şekilde,

yüksek konsantrasyonlarda, ATP moleküllerinin kendi kendine birleşmesinin, daha büyük PNIPAM agregatlarının daha küçük olanlara doğru kısmen dengesizleşmesine yol açtığı gözlemlenmiştir. ATP bağlanma bölgelerinin yokluğunda, rastgele halka benzeri yapılı makromoleküllerle etkileşimler, ATP'nin hidrotropik etkisine yol açmaz. Bunun yerine, ATP molekülleri makromolekülleri çözmekten ziyade stabilizatör olarak işlev görürler.

*Anahtar Kelimeler:* Adenozin trifosfat, adenozin monofosfat, tripolifosfat, adenin, adenosin, hidrotroplar, ısıya duyarlı polimerler, PNIPAM, PDEA

# ACKNOWLEDGEMENT

First and foremost, I extend my sincere gratitude and immense thanks to my advisor, Dr. Halil Ibrahim Okur, for his unwavering support, patient guidance, and belief in me from day one. His mentorship not only broadened my academic horizons but also transformed my overall experience, allowing me to explore new possibilities and overcome challenges beyond my initial expectations. It is a true privilege to be mentored by him.

I would like to thank Dr. Aykut Erbas for serving on my thesis committee, co-guiding my research, and providing valuable feedback for my thesis. I would also like to thank Dr. Sreeparna Banerjee, for kindly agreeing to be a part of my committee and editing my thesis. I want to thank BAGEB for providing financial support for this research.

I am delighted to be part of the Okur Research Group, where the members have shown remarkable friendship, support, and assistance. Thanks to Yaren, Ertan, Sobia, and Sena for fostering the best possible lab environment. Special appreciation to alumni, Dr. Ezgi Yılmaz, Umay, Dilşad, and Ferhat, for sharing their knowledge with me. Additionally, thanks to Erbas Research Lab members Ata and Göktuğ for their valuable contributions.

I would like to extend my special thanks to both the members of the Chemistry department at Bilkent University and all my friends within the department.

Bilkent and Ankara became a warm and welcoming home, thanks to my wonderful friends: Melis, Arçin, Güneş, Kutay, Eylül, Pedram, Umut and Aydamir. I feel exceptionally fortunate to have such amazing friends who made my time truly special.

My heartfelt gratitude is reserved for my family, for their constant presence in my life, for guiding me to my current place, and for the colors they have brought into my life. And Gün, thank you for turning each chapter into a beautiful melody in this adventurous journey.

# Contents

# List of Figures

# LIST OF ABBREVIATIONS AND SYMBOLS

| | |
|---|---|
| ATP | Adenosine Triphosphate |
| AMP | Adenosine Monophosphate |
| TP | Tripolyphosphate |
| ATP / derivative | ATP and ATP derivatives such as adenine, adenosine, triphosphate, and adenosine monophosphate |
| IDP | Intrinsically Disordered Protein |
| LCST | Lower Critical Solution Temperature |
| ATR-FTIR | Attenuated Total Reflectance Fourier Transform Infrared spectroscopy. |
| NMR | Nuclear Magnetic Resonance |
| MD | Molecular Dynamics |
| MCR | Multivariate curve resolution |
| SMCR | Self-modeling curve resolution |
| NaXS | Sodium Xylene Sulfonate |
| ELP | Elastin-like Polypeptide |

# Chapter 1 - Introduction

## 1.1 Aqueous Phase Behavior of Biomacromolecules

*The solution phase behavior of biomacromolecules leads to life*. Biomacromolecules, including proteins, nucleic acids (DNA and RNA), carbohydrates, and lipids are large molecules found in living organisms. When these biomacromolecules are in a solution (usually in an aqueous medium, as it's the primary solvent in biological systems), they exhibit various behaviors. Common behaviors include solubility, conformational changes, hydration, aggregation, ionization, enzymatic activity, and denaturation. The behavior of biomacromolecules in solution depends on the specific characteristics of the molecule and the environmental conditions. Understanding these behaviors helps elucidate how biomacromolecules function in living organisms and various laboratory applications. This chapter focuses on biomacromolecules and explores the factors influencing their behavior in the solution phase. It then delves into the current molecular-level understanding of specific ion and osmolyte effects on macromolecules in aqueous solutions, contextualizing the relevance and motivation of this present thesis study, as detailed in the following sections.

Biomacromolecules have varying solubilities in water. Protein solubility, for instance, can be impacted by a variety of factors. Temperature[1,2], ionic strength[3], pH[4], and the existence of different solvent additives are examples of extrinsic variables that affect protein solubility. [5] These variables can be adjusted to get a high solubility[5–8], but changing the solution conditions isn't always sufficient to raise the necessary level of protein solubility. For example, the solubility of PNIPAM, poly (*N*-isopropyl acrylamide), was studied in aqueous solutions with a series of nine different cation chloride salts. The study[9] revealed that all cations were

generally depleted from the macromolecule/water interface, but strongly hydrated cations could accumulate around the amide oxygen. The dominating salting-out effect decreased to a greater extent with increasing salt concentrations because of these weak but favorable interactions. Moreover, the amino acids consisting of the protein, especially the ones located at the surface of the 3D structure determine the intrinsic features that affect solubility. [10–12] Yet, there remains a lack of comprehensive knowledge regarding how to modify the inherent properties of a protein to enhance its solubility.[5,8,13]

The inter and intra-molecular interactions between biomacromolecules are generally facilitated via Coulomb (ionic) interactions; hydrogen bonds[14], ionic interactions, van der Waals forces, and hydrophobic interactions[15]. These interactions are essential to various biological functions, such as enzymatic catalysis[16], cell signaling, protein folding[17], membrane transport[18], immune responses, and metabolic pathways[19]. Some biomacromolecules also participate in chemical reactions in solution. For instance, enzymes catalyze biochemical reactions by binding to substrate molecules and facilitating their conversion into products. They require specific metal ions (cofactors) to function. The identity and concentration of these metal ions in the solution became critical for the activity of such biomacromolecules.

Water is a fundamental building block of life, and most biological processes take place in an aqueous environment. [20] In this context, the water environment can have a significant impact on the structure and functionality of biomolecules immersed within it. [21,22] Biomacromolecules surrounded by water molecules in solution create a hydration shell. This hydration shell reduces the interactions between hydrophobic regions and water, providing stability to the macromolecule. The hydration shell concept has been employed to uncover the distinctive properties of water next to biomolecules and molecular assemblies such as

membranes.[23,24] The hydration shell in a qualitative perspective is made up of the first (or the first few) water layer that surrounds the biomolecule and interacts with it. [25] However, the aqueous environment "sufficiently" away from the biomolecular surface ought to exhibit characteristics of bulk water. [25] The separation of the hydration shell from bulk water presents significant hurdles from the perspectives of both structure and dynamics. While there is comprehensive knowledge regarding the structure and dynamics of bulk water, the understanding of water behavior within hydration shells is notably limited. There are different ideas about how water behaves near a biomolecule and the extent to which the water structure around it differs from bulk water. [25] The main issues are outlined below:

First, a biomolecule's surface, being nonplanar and corrugated, sets steric conditions for the nearby hydration shell. This results in a distinct spatial arrangement of water molecules from bulk water in the initial hydration layer, impacting their vibrational and rotational properties. [26–29] Gradually, the hydration shell absorbs the bulk water structure as it moves from the initial water layer to farther distances from the biomolecular surface. The scale of this structural adaptation is debated, with estimates ranging between 2 and more than 10 water layers.

Secondly, polar and charged groups on biomolecule surfaces interact with the initial water layer through electric forces and local hydrogen bonds, influencing the structural diversity of hydration layers. [26,30] The strength and spatial extent of these electric fields, as well as the occurrence and strength of hydrogen bonds between hydrating water and the biomolecule, remain poorly characterized. Diverse interactions, including strong hydrogen bonds and clathrate water structures, contribute to temporal variations in hydration shell dynamics, exhibiting behavior distinct from bulk water and awaiting precise quantification.

Moreover, debates arise about the behavior of water molecules inside a hydration shell. One viewpoint proposes a more rigid water structure with reduced fluctuations and increased hydrogen bond lifetimes, termed "biological water." [31,32] However, recent molecular-level simulations and experimental studies contradicted this concept, suggesting only a moderate slowdown in water dynamics, typically by factors of 2 to 3 compared to bulk water.[33–35]

Finally, the detailed examination of hydration shell dynamics is often justified by their presumed influence on biomolecular conformational dynamics. While water is commonly seen as a lubricant of biomolecular motions [22,36], recent studies present conflicting perspectives. Beyond affecting biomolecular flexibility, hydration shell dynamics are suggested to be crucial for biomolecular function, influencing activities like protein anti-freeze capabilities and enzyme catalysis. Despite the belief in a minimum hydration level for protein functionality (approximately 0.3 g of water per gram of protein), experimental evidence challenges this notion, raising questions about the strict necessity of a dynamic hydration shell for biomolecular function. The findings have demonstrated that enzyme proteins can maintain their flexibility and functionality at low humidity levels (below 0.03 g of water per gram of protein) and when water is substituted with an organic solvent.

Biomacromolecules, such as proteins and nucleic acids, contain ionizable functional groups (e.g., amino acids in proteins with acidic and basic side chains). The pH of the solution can influence the ionization state of these groups. For example, at low pH, basic groups tend to be protonated, while at high pH, acidic groups tend to be deprotonated. Changes in pH can also induce conformational changes in biomacromolecules.[37] For instance, proteins may fold or unfold in response to changes in pH. Shang et al. investigated the effect of pH on the conformational changes of Bovine Serum Albumin (BSA) in the bioconjugates, and the

outcomes revealed that the pH dependency might stem from the intrinsic conformational state adopted by albumin at various pH levels. [38]

Lastly, temperature and salt (ion) concentration are two additional factors that can impact the conformational changes [39–44] and the behavior of biomacromolecules. Different ions have distinct abilities to precipitate proteins from a solution, as indicated in the Hofmeister series of cations and anions. [45] For example, certain ions can stabilize the structure of proteins (e.g. $SO_4^{2-}$), while others can disrupt it (e.g., chaotropic ions like guanidinium chloride). Before diving into the details, it's important to introduce the historical studies on ion-specific effects on proteins, which originated in Prague in the 1880s and were led by Franz Hofmeister.

## 1.2 Effect of Ions on Biomacromolecules: The Hofmeister Series

The ion-specific effects on macromolecules have been a major focus in understanding the solution phase behavior of macromolecules and attaining a molecular-level understanding of the Hofmeister series. [5,7,46–58] Concerning ion-specific effects on proteins will be elaborated, guiding the reader through the developments, that eventually led to today's molecular-level understanding of the Hofmeister series. Hofmeister and his collogues compiled their studies on ion-specific effects in a series of seven articles published in German literature from 1887 to 1898. His comprehensive investigations into the salting-out of proteins were remarkable in several aspects. He pioneered the systematic quantification of salting-out effects across a complete set of salts, a compilation later recognized as the Hofmeister series, which was initially reported in 1888. [45] The relative influence of ions on the physical behavior of a wide range of aqueous processes, from protein folding to colloidal assembly, is ranked using this

Hofmeister series. Furthermore, his work with the various sets of salts that share a common cation or anion enabled the construction of a separate Hofmeister series for cations and anions.

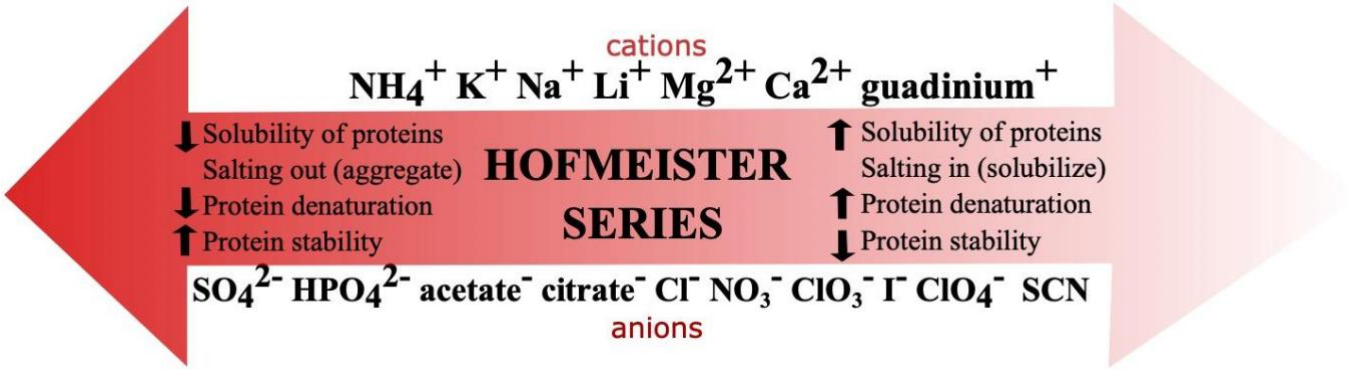


**Figure 1.1:** The Hofmeister series for cations and anions. (Inspired from ref [44])

Hofmeister's first study appeared a few years after Arrhenius' discovery that salts dissociate into ions in water.[59] Following this, he published his second paper titled "About regularities in the protein precipitating effects of salts and the relation of these effects with the physiological behavior of salts" [45] and his third paper titled "About the water withdrawing effect of the salts" [60], which are among his most significant works. Hofmeister's objective was to classify the salts and the species that are salted out and included a range of proteins as well as other substances such as sodium oleate, gelatin, and colloidal ferric oxide. [45] In the original work, Franz Hofmeister investigated the solubility of egg-white proteins in various aqueous salt solutions at different salt identities and concentrations. Based on these studies, he proposed a diverse "water-withdrawing effect" of different salts, attempting to establish a direct link to their salting-out abilities. [45]

The typical ion ordering of the anionic series is shown below:

$CO_3^{2-} > SO_4^{2-} > S_2O_3^{2-} > H_2PO^{4-} > F^- > Cl^- > Br^- > NO_3^- > I^- > ClO_4^- > SCN^-$

The ionic species located to the left of $Cl^-$ are termed kosmotropes, or historically considered as 'water structure makers'. They are highly hydrated and exert stabilizing effects, leading to the salting-out phenomenon in macromolecules. Proponents of the concept of "kosmotropes" and "chaotropes" later embraced Hofmeister's idealistic objective of explaining particular ion effects on general solutes in terms of the interactions of salt ions with water. This theory states that the former group of ions, such as $SO_4^{2-}$ or $F^-$, are successful at salting out because they provide order (kosmos) to the solution and may arrange several layers of water molecules around themselves. On the other hand, the species to the right of $Cl^-$ such as $SCN^-$, $ClO_4^-$, or $I^-$, cannot organize water molecules around them and are hence ineffective as salting out agents. They are termed chaotropes and traditionally identified as 'water structure breakers'. Known for their ability to destabilize folded proteins, they consequently exhibit salting-in behavior.[8] While the interpretation of the Hofmeister phenomenon may appear to offer a simple, broad overview, the structure-maker vs. structure-breaker paradigm for explaining Hofmeister's effects began to change in the late 20th century. The suggested characteristic of the various ions in the series, leading to the terms kosmotrope and chaotrope, faced challenges in being supported by experimental evidence. As spectroscopic and thermodynamic tools improved, studies started to reveal that ions did not seem to alter the structural order of water beyond their immediate solvation shells. It was recognized that the impact of ions in the bulk did not provide a strong enough explanation for the origin of the Hofmeister series. [5,44,46]

Bakker and coworkers conducted a series of studies in this regard.[61–66] They utilized femtosecond pump-probe spectroscopy to measure the orientational time of water molecules in a salt solution containing $Cl^-$, $Br^-$, $ClO_4^-$, or $SO_4^{2-}$. Ultrafast infrared irradiation excited O-H stretching modes, followed by a weaker IR pulse to monitor relaxation behavior with high time resolution. The presence of both kosmotropic and chaotropic ions increased correlation times for water molecules in the first hydration shell, especially for anions. Nevertheless, neither class of ions influenced bulk water dynamics indicating unaffected bulk water structure. Pielak and coworkers investigated the impact of stabilizers and denaturants, such as sugars, guanidinium salts, and urea, on proteins using pressure perturbation calorimetry.[67] They converted their experimental data to the pressure dependence of the partial heat capacity to investigate the effect of stabilizers and denaturants on water structure by utilizing the classical two-state mixture model for water. In contrast to commonly held assumptions, their study revealed no connection between the type of solute and its role as a water structure maker or breaker in bulk water. [67] Finally, Cremer and coworkers utilized surface-selective vibrational sum frequency spectroscopy (VSFS)[68–70] to demonstrate the Hofmeister effect in an octadecyl amine monolayer spread on salt solutions. The findings showed that the disruption of the alkyl chain region by an anion aligns with the Hofmeister series, indicating that dispersion forces play a crucial role in this effect. In contrast, the impact of ions on hydrogen bonding and the structure of interfacial water was less straightforward.[67] Consequently, it was understood that the concepts of “kosmotropes" and "chaotropes" do not work for making or breaking water structures. Furthermore, extensive evidence from nature itself showed that salting out behavior cannot be properly explained by only considering ions and water; rather, the protein solute must be explicitly taken into consideration. Lysozyme,

for example, salts out of solution according to the Hofmeister series exclusively at high pH levels and ionic strength. However, under neutral and acidic conditions, it follows a reversed Hofmeister series. [71–73]

Overall, to enhance our understanding of the Hofmeister series, it is crucial not only to understand the hydration properties of salt ions but also to delve into their interactions with protein surfaces. Following this realization in the 1960s, the so-called Renaissance period of the Hofmeister series began. The studies[74–76] from this period probed various thermodynamic and spectroscopic techniques, which mainly examined the protein backbone, and showed that the amide group interacts preferentially with strongly hydrated cations (such as $Li^+$, $Mg^{2+}$, or $Ca^{2+}$) and weakly hydrated anions (such as $Br^-$, $I^-$, $ClO_4^-$, or $SCN^-$). Simple thermodynamic considerations imply that salting in and instability of the protein are caused by attractive ion-backbone interactions. This suggests that ions that are firmly partitioned to the protein surface have a reduced capacity for salting out (and stabilizing), which aligns the aforementioned findings with the Hofmeister series.

While the intricate molecular mechanisms of ion-macromolecule interactions have been demonstrated for Hofmeister ions[13,77–81], the specific molecular-level intricacies concerning how small molecules and osmolytes impact the macromolecules within the aqueous environment remain incompletely understood. In the following section, the effects of small molecules including osmolytes on biomacromolecules will be detailed.

## 1.3 Small Molecules: Effect of Osmolytes on Biomacromolecules

Small molecules refer to organic compounds with a relatively low molecular weight (<1000 daltons). [82] These compounds are typically around 1 nm in size and have the remarkable capacity to regulate biological processes. They can act as inhibitors or activators, modulating the activity of biomacromolecules. For instance, competitive inhibitors compete with natural substrates for binding sites on enzymes, while activators enhance enzymatic activity. Additionally, they play a critical role in regulating macromolecular interactions, modifying the affinity between molecules, and disrupting non-covalent bonds. Ligands, for instance, can bind to biomacromolecules, which can then cause conformational changes and control biomacromolecules' activity. [10] This is particularly important in the context of enzymes, receptors, and transport proteins. Small molecules like metabolites (e.g., ATP, NADH) serve as substrates, cofactors, and regulators in various biochemical pathways, influencing the behavior of biomacromolecules involved in these pathways. Another important aspect of small molecules is their involvement in the regulation of gene expression[83–85], affecting processes such as transcription [86–88], translation[89], and the stability of RNA and proteins involved in gene regulation [90]. Their diverse effects on macromolecules are crucial for maintaining cellular homeostasis and are essential for signal transduction, metabolism, and the immune response. Investigating and understanding these molecular interactions not only advances our knowledge of biomolecular systems but also offers potential avenues for therapeutic interventions.[91,92]

Osmolytes (organic osmotic solutes) are small organic molecules observed in bacteria, plants, and animals. The osmolyte systems commonly found in water-stressed organisms include polyhydric alcohols, free amino acids along with their derivatives, and combinations

of urea and methylamines.[93] These types of osmolytes are present in nearly all organisms under water stress [93,94]. The use of organic osmolyte systems has two primary advantages: their compatibility with macromolecular structure and function at high osmolyte concentrations, and the reduced necessity for protein modification to function effectively within concentrated intracellular solutions. [93] In aqueous environments, osmolytes have been categorized as "stabilizers" due to their capacity to enhance the stability of proteins and other large biomolecules. They favor the folded (or native) state over the unfolded state of the concerned protein in the equilibrium between Unfolded ⇌ Folded. Another category of osmolytes is referred to as "denaturants", and they have the opposite effect on biomacromolecules. These osmolytes induce the denaturation of proteins and/or large biomolecules in aqueous solutions, favoring the unfolded state over the native state of the target proteins[94,95]. It's important to note that stabilizer osmolytes and stabilizing (salting-out) ions exhibit comparable effects on proteins. Such similarities are also seen between destabilizing (salting-in) ions and denaturant osmolytes.

Urea and guanidinium ion ($Gnd^+$) are among the most well-known osmolytes capable of denaturing various proteins. They have been studied in the literature for more than 60 years, exploring both direct interactions with the protein backbone and side chains, as well as direct effects resulting from the interaction with water molecules. [96–99] Guanidium was demonstrated to exhibit a preference for charged residues, and its charge delocalization leads it to stack with aromatic side chains such as tryptophan, phenylalanine, tyrosine, and histidine within proteins' interior, thereby playing a substantial role in the unfolding of the protein. [100,101] Urea, aside from binding with charged and polar residues, has a notable impact on polar interactions

within the protein backbone by binding to carbonyl oxygen, leading to the destabilization of secondary structure elements. [101–103]

Several attempts were made to elucidate the denaturant effect of guanidium on proteins. [96–99] However, these investigations did not suffice to offer a molecular-level explanation. As research tools have advanced in the last few decades, numerous studies have delved into a detailed exploration of the denaturant effect of guanidinium. These investigations include MD simulations [104–106], thermodynamic measurements [104], and spectroscopic analyses. [104,106] Heyda et. al utilized a combination of experimental techniques (circular dichroism (DS), differential scanning calorimetry (DSC), and NMR) along with MD simulations to investigate the denaturation of the Trp-cage mini protein by guanidinium and urea.[106] The destabilizing effect of both urea and guanidinium on Trp-cage was remarkably similar, despite their distinct interactions with proteins.[106] Okur et al. performed a combination of phase transition and FTIR measurements together with MD simulations to elucidate how guanidium (Gnd+) salts impact the stability of the collapsed and uncollapsed states of an elastin-like polypeptide (ELP), a thermoresponsive polymer. [104] The research revealed that guanidium's action was influenced by the specific counter anion it was paired with. When paired with well-hydrated anions like $SO_4^{2-}$, guanidium was depleted from the ELP/water interface, stabilizing the collapsed state through an excluded volume effect. At low salt concentrations, guanidium also stabilized the collapsed state when paired with $SCN^-$, a strong binder for the ELP. In this scenario, both the cation and anion were concentrated in the collapsed state of the polymer. This effect was attributed to guanidium's capacity to facilitate cross-linking of polymer chains. However, at high salt concentrations, guanidium began to stabilize the uncollapsed state. This shift occurred because, at this concentration (>1.5M), both the anion and the cation were present in

sufficient amounts to partition to the polymer surface, preventing the formation of cross-links. Moreover, the salts having an intermediate interaction with the ELP, such as GndCl, exhibited a preference for the uncollapsed conformation at all salt concentrations. The findings offer a comprehensive molecular-level understanding of how $Gnd^+$ impacts the stability of polypeptides, shedding light on the conditions in which guanidium salts can serve as potent and versatile protein denaturants.

Achieving molecular level detailed mechanisms of osmolytes affecting the stability of proteins and (bio)macromolecules in aqueous medium concerning several factors (e.g., temperature, pH, humidity, concentration, osmotic pressure, etc.) is quite important. This is simply due to the natural presence of osmolytes in the cytosol and extracellular fluid of numerous organisms; fungi, protozoa, multicellular algae, vascular plants, insects, cartilaginous fishes, amphibians, and even mammalians including humans [93,94] As a consequence, it is vital to investigate osmolytes and their behavior in full-scale, since a variety of protein-related disorders are shown to cause by protein misfolding, protein aggregation (e.g., Alzheimer, and Parkinson) or conformational abnormalities, which can play an important role in the pathogenesis of amyloid-related diseases and pose a significant barrier to the production and development of protein therapies [93,107–112]

## 1.4 Hydrotropes

In 1916, the German chemist Carl Neuberg authored a publication discussing what he referred to as “hydrotropic appearances”.[113] He was describing the strange effects that small organic salts had on the solubility of compounds that would otherwise be insoluble. Since then, the term “hydrotropy” has gained widespread recognition in the field and continues to

be used today. To provide a contemporary definition, a hydrotrope is a compound that doesn't form aggregates on its own (unlike surfactant). Instead, they are small molecules that increase the solubility of poorly soluble compounds in aqueous solutions.[114–119] They possess both hydrophilic and hydrophobic components, similar to surfactants. However, they differ from surfactants in that they typically have shorter alkyl tails or aromatic rings, which prevent spontaneous self-aggregation. [119] The hydrophilic part generally has a relatively less impact on hydrotropic behavior, while the hydrophobic portion typically results in increased hydrotropic efficiency [112]. In Neuberg's initial publication on this matter, he addressed various aspects that later became significant in hydrotrope science. Specifically, he mentioned that pentyl and benzyl sulfate do have hydrotropic characteristics, while ethyl sulfate does not. He pointed out that 5 to 6 carbon atoms appear to be the optimum. This observation emphasizes a fine balance between the ionicity of the headgroup and structural hydrophobicity, a topic also the subject of a recent publication. [120] Neuberg also observed the effects of hydrotropes on inhibiting the formation of liquid crystals. This aspect was extensively examined by Friberg et al. after around 70 years. [121] While certain observations made by Neuberg have only recently become well-established (such as the "pre-ouzo" effect), his visionary endeavor to utilize hydrotropes for pharmaceutical solubilization endures, and his concept continues to be applied in the pharmaceutical industry to this day. Additionally, he also documented the solubilization of proteins with hydrotropic salts, which aligns thematically with Franz Hofmeister's prior work on protein solubility. However, while Hofmeister concentrated on the salting-in and salting-out effects of inorganic salts, Neuberg conducted experiments on the solubilization of proteins.[45] He examined their behavior, particularly during heating, and discriminated the apparent "salting-in" effect of his recently discovered hydrotropes from the effects observed

for typical salting-in ions such as thiocyanate (later referred to as “chaotropes”). He recognizes the similarities in protein solubilization but highlights distinctions in the solubilization of aliphatic/hydrophobic compounds. This correlation has recently reemerged in publications discussing a suggested hydrotropism for ATP. For example, according to a recent study by Patel et al.[122], ATP can operate as a biological hydrotrope to maintain protein solubility and suppress macromolecule aggregation. While this concept has been supported by a large body of research, there are just as many that argue that ATP does not act as a hydrotrope. Conflicting theories on ATP's hydrotropic nature are proof that the concept of hydrotrope is not yet wholly grasped. Consequently, gaining a comprehensive understanding of the hydrotropic mechanism has proven to be a challenging task.

### 1.4.1 Adenosine Triphosphate (ATP) as a Biological Hydrotrope

The human body is an intricate and complex organism that requires energy to maintain its proper functioning. At the cellular level, adenosine triphosphate (ATP) serves as the primary energy source, driving biochemical reactions within cells, and functioning as a signaling molecule in both extracellular and intracellular signaling cascades. It also facilitates both immediate utilization and storage, details of which have been extensively described elsewhere.[123–129] Referred to as the "energy currency" of the cell, ATP possesses easily releasable energy within the bond connecting the second and third phosphate groups. Apart from supplying energy, the hydrolysis of ATP plays a crucial role in numerous cellular functions, such as signaling and DNA/RNA synthesis. The synthesis of ATP relies on the energy derived from various catabolic processes, including cellular respiration, beta-oxidation, and ketosis.[130]

ATP has a structure known as a nucleoside triphosphate, consisting of a nitrogenous base (adenine), a ribose sugar, and a series of three phosphate groups linked together. Having both the hydrophilic (through the triphosphate moiety) and relatively hydrophobic (via the adenine base) groups together, ATP has an amphiphilic nature. Due to its amphiphilic property, it has the general characteristics of a hydrotrope but does not assemble into structures such as micelles. The structure of the ATP molecule can be seen in Figure 1.2.

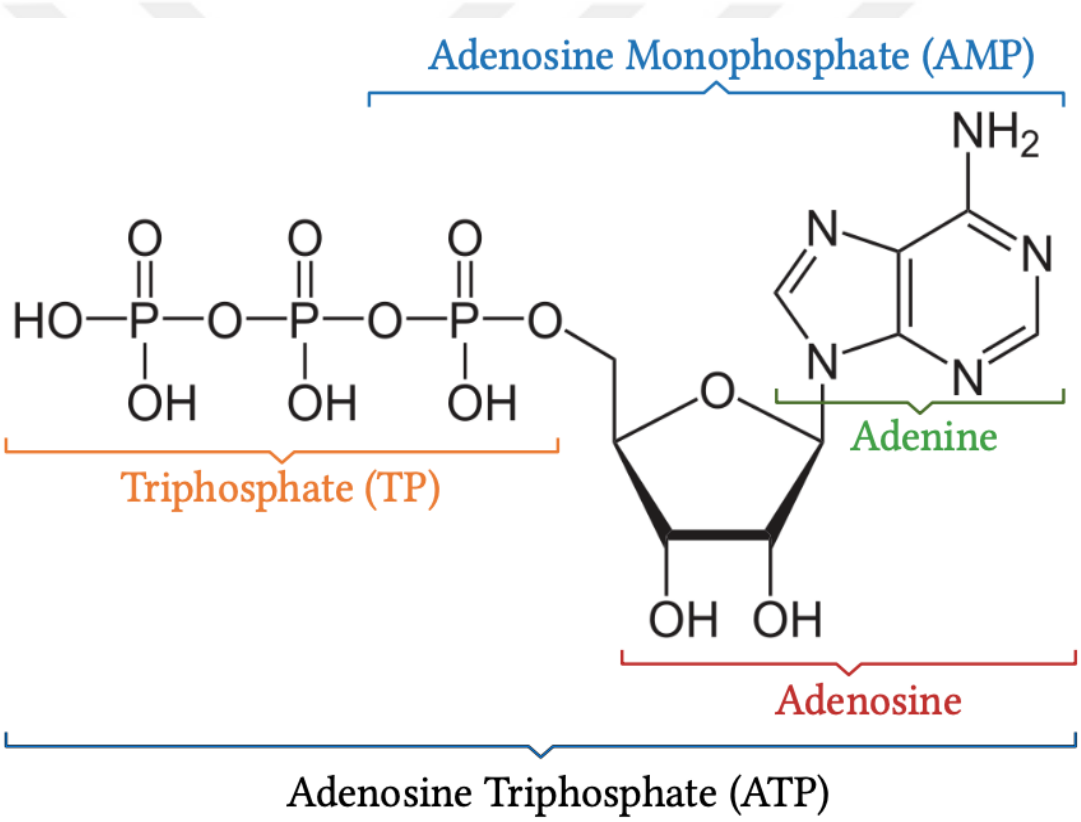


**Figure 1.2:** The structure of the Adenosine triphosphate (ATP) molecule includes its components: adenine, adenosine, triphosphate (TP), and adenosine monophosphate (AMP).

In general, cells maintain an ATP concentration of 1-10 mM, far greater than what is needed to sustain metabolic activity. Its concentration might reach relatively high levels in specific regions, e.g., 0.1 mM within the chromaffin granules of the adrenal medulla. [122,131–

[133] It has recently been proposed that ATP is not only involved in the formation of membranelles organelles through liquid−liquid phase separation (LLPS) which permits temporal and spatial control over intricate metabolic processes [134,135], but also influences the development of some illnesses, such as cancer, neurological disorders, and even viral infections [136,137], by modifying the activity of LLPS or preventing the fibrillation of the proteins that cause these conditions. [138–140] More importantly, it has been reported that ATP functions as a biological hydrotrope, as was already indicated in section 1.4. This surprising finding suggests an additional role of ATP in preserving protein solubility, preventing protein aggregation, and dissolving liquid-liquid phase separation (LLPS) of intrinsically disordered proteins, including FUS, TAF15, hnRNPA3, and PGL-3, within biological systems. [122] In a similar spirit, it was discovered that a high concentration of ATP is upheld in the metabolically quiescent organ, the eye lens, to avoid the crowding of γS-Crystallin. [141] There is also evidence supporting the ATP-driven solubilization of aggregates in Xenopus oocyte nucleoli.[142] Additionally, a comprehensive proteome profiling analysis proposed that ATP plays a role in regulating the solubility of a considerable number of proteins.[143] The majority of these recent studies have led to the introduction of a novel role for ATP as a "biological hydrotrope." In contrast, a subsequent study [144] presented an argument that although ATP reduces protein aggregation, this mechanism cannot be ascribed to classical hydrotropic effects. Instead, the inhibition of fibrillation in disordered proteins was attributed to specific interactions between adenosine and aromatic amino acid side chains. [144] Therefore, with a wealth of experimental evidence reinforcing ATP's hydrotropic effect, several studies propose refraining from classifying ATP as a conventional hydrotrope. This intensifies the debate on this matter and underscores the importance of scientific scrutiny in this regard.

Examining prior research in this field reveals that a significant majority has concentrated on ATP's effect on intrinsically disordered proteins or natively folded proteins. ATP is recognized for its binding affinity to RNA recognition motifs within RNA binding proteins and RGG low-complexity domains (LCDs) present in intrinsically disordered proteins. [145–149] However, ATP interactions extend beyond the binding sites for nucleic acids on proteins. A proteome-wide study revealed that roughly a quarter of the insoluble proteome in human Jurkat cells is solubilized by ATP. [143] Notably, only a small fraction of the solubilized proteins are known to bind ATP, while the majority consists of proteins containing intrinsically disordered regions abundant in basic amino acids. The HSQC-NMR analysis has identified the binding to an arginine-enriched IDR region of TDP-43, yet no direct binding has been observed for the arginine-rich globular eye lens protein γS-crystallin[141], which suggests that flexibility or disorder is a key factor in determining the binding propensity. However, this doesn't imply that binding doesn't take place in proteins that are natively folded. Nishizawa et al.[150], identified multiple ATP binding sites using NMR on ubiquitin and ubiquitin domain-associated receptor p62 (UBA) within flexible protein regions enriched in basic and hydrophobic residues. According to 1H−15N HSQC experiments, changes in amide chemical shifts were observed in resonances associated with the main hydrophobic surface of Ub (T9, I44, H68, and V70). ATP associates with Ub by forming noncovalent weak interactions primarily involving hydrophobic and basic amino acids, particularly those around the I44 hydrophobic patch, including V70[150]. Specifically, binding occurs with the C-terminal tails for both proteins and the loop region of ubiquitin. In the case of positively charged proteins such as lysozyme and the IDP histatin-5, low concentrations of triphosphate have the opposite effect of inducing protein precipitation[151,152]. Likewise, ATP has been demonstrated to

enhance fibril formation in various basic IDPs [153], along with an insulin fragment conjugated to octalysine[154]. In each of these cases, the ion-specific effects were attributed to polyphosphate, which creates ionic bridges between the basic groups of proteins.

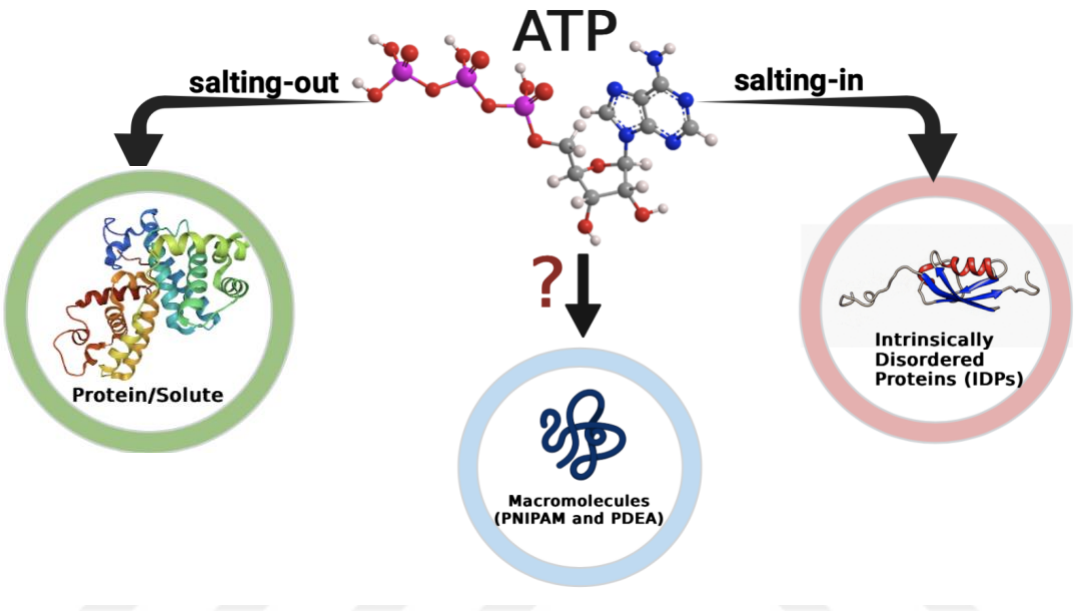


**Figure 1.3:** Salting-in and salting-out behavior of Adenosine triphosphate (ATP) on natively folded and intrinsically disordered proteins, respectively.

Overall, ATP primarily stabilizes natively folded proteins through a salting-out effect, while preventing the fibrillation of intrinsically disordered proteins (IDPs) by exhibiting a salting-in behavior, as illustrated in Figure 1.3. Given that ATP binds to valine (V70) which is the main hydrophobic surface of ubiquitin, we anticipated a similar interaction between ATP and a model macromolecule having a chemical structure resembling proteins and a random-coil structure similar to intrinsically disordered proteins (IDPs). The question was: How does ATP interact with a model macromolecule possessing characteristics bridging the gap between these two types of proteins?

In this context, Poly (*N*-isopropyl acrylamide) (PNIPAM) proves to be a suitable macromolecule for our research purposes due to the isopropyl group in its structure,

resembling that of Valine. Moreover, PNIPAM lacks a well-defined three-dimensional structure, and in a random coil, the polymer chain does not adopt a specific repeating pattern or secondary structure, such as an alpha helix or beta sheet observed in proteins. Therefore, PNIPAM exhibits physical characteristics akin to IDPs. Overall, it possesses traits between natively folded proteins and IDPs. The subsequent section will provide detailed information on the model macromolecules employed in the forthcoming experiments.

## 1.5 Model Systems

Poly (*N*-isopropyl acrylamide) (PNIPAM) is a well-established temperature-responsive polymer that was initially synthesized in the 1950s and remains one of the most extensively investigated and widely used smart polymers to this day.[5,155,156] PNIPAM undergoes a sharp coil-to-globule transition at temperatures above its lower critical solution temperature (LCST), which is approximately 305 K in water. [8] This behavior is analogous to the phenomenon of cold denaturation observed in proteins.[157]

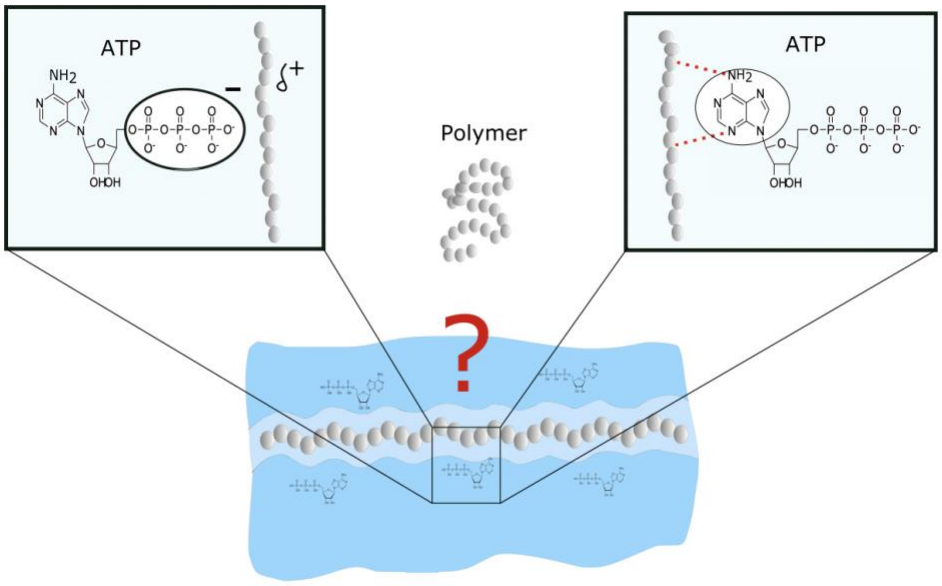


**Figure 1.4:** The possible interaction mechanism between ATP and macromolecules (indicated with gray beads) involving two pathways: (left) interaction with the tripolyphosphate group, or (right) electrostatic interactions between adenine/adenosine and the macromolecule.

Furthermore, the structure of PNIPAM (Figure 1.5, *left*) includes various hydrophobic elements such as backbone groups and the isopropyl group on the sidechain, as well as hydrophilic components like the amide group on the sidechain. This arrangement mimics the hydrophilic peptide groups and the hydrophobic side-chain groups of natural proteins. The coexistence of groups with diverse chemical environments and hydrophobicity levels makes PNIPAM-type polymers perfect for studying how the polarity of the polymer groups affects preferred interactions with ions. The temperature-dependent characteristics of PNIPAM can be attributed to the combination of hydrophilic amide groups, a hydrophobic backbone, and isopropyl moiety. Below the LCST, the dominant hydrogen-bonding interactions between the hydrophilic groups of PNIPAM and water enforce a coil-like conformation in the polymer. [158] Above the LCST, the solvation entropy of the hydrophobic groups in both the backbone and side chain becomes dominant. Consequently, PNIPAM undergoes a transition from a coil-like conformation to a compact globule-like structure in aqueous solution. [159]

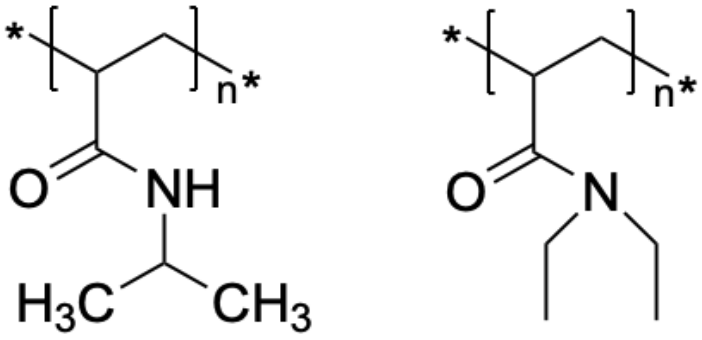


**Figure 1.5:** *(left)* The structure of Poly(N-isopropyl acrylamide) (PNIPAM), *(right)* the structure of poly(N, N- diethyl acrylamide) (PDEA) polymers.

To ensure the experimental rigor, another macromolecule poly (*N*, *N*- diethyl acrylamide) (PDEA) was utilized. This macromolecule shares a similar structure to PNIPAM, thereby strengthening the robustness of the investigation (Figure 1.5, *right*).

# Chapter 2 – Materials and Methods

## 2.1 Materials

The chemicals used in this study are listed below with the percent purity listed in parentheses. Poly (*N*-isopropyl acrylamide) (PNIPAM) (Polymer Source, Inc., 118.500 g/mol), poly(*N*-isopropyl acrylamide) (PNIPAM) (Sigma Aldrich., 85.000 g/mol), poly(*N, N*- diethyl acrylamide) (PDEA) (Polymer Source, Inc., 55.000 g/mol), adenosine (Sigma Aldrich, 99% purity), adenine (Sigma Aldrich, 99% purity) sodium triphosphate pentabasic (Sigma Aldrich, 98% purity), adenosine 5'-triphosphate disodium (ATP) (Sigma Aldrich, 99% purity), adenosine 5'- monophosphate sodium salt (Sigma Aldrich, 99% purity), sodium xylenesulfonate (NaXS) (Sigma Aldrich, mixture of isomers, 40 wt. % in $H_2O$), $H_2O$ (Millipore Nanopure system, 18.2 M cm), deuterium oxide ($D_2O$) (Eurisotop, 99.90% D) were used without any further purification.

## 2.2 Sample Preparation

Lyophilization, also known as freeze-drying, is a process of removing solvent, i.e. water, from a substance by freezing the polymer solution at low temperature and subsequently subjecting it to a vacuum. To perform lower critical solution temperature (LCST), ATR-FTIR, and NMR measurements with precision, it is crucial to have polymer samples of the utmost purity. This method plays a crucial role in achieving this goal by removing the residual solvent or moisture present in the sample, resulting in a dry and stable polymer sample. [160]


**Figure 2.1:** The setup for the vacuum-drying process. The desiccator (on the right), and the vacuum pump (on the left).

To begin with, an accurate mass (with four significant figures) of the solid polymer (PNIPAM or PDEA) was measured and dissolved in deionized water within 10 mL volumetric flasks, resulting in a final concentration of 20 mg/mL and 5mg/ml stock solutions. The preparation of samples involved transferring desired volume aliquots of the stock solution into Eppendorf tubes using a micropipette. Specifically, for the LCST measurements, the Eppendorf tubes were filled with 100 μL of the 5mg/ml stock solution, and 100 μL of the 20mg/ml for ATR-FTIR measurements. Special care was taken during the transfer of the aliquot to the bottom of the Eppendorf tubes to ensure that no solution droplets remained on the Eppendorf tube walls. This was crucial as any residual solution on the walls could lead to the formation of solid residue during the subsequent vacuum drying process. The Eppendorf tubes were sealed using punctured lids to allow for the effective removal of moisture from the

samples and facilitate the drying process induced by the vacuum during lyophilization. Separate lids were used for each set of polymer samples to avoid any cross-contamination. The prepared samples were immersed in liquid nitrogen for at least 10 minutes for a complete freezing process. Subsequently, the tubes were carefully removed from the liquid nitrogen and promptly placed in an upright position inside an Eppendorf storage box to prevent any melting of the samples at room temperature. Lastly, the Eppendorf storage box was placed inside a desiccator, and the samples were subjected to vacuum drying overnight. Once the vacuum drying was complete, the samples were taken out of the desiccator and stored in a refrigerator to later utilize for LCST and ATR-FTIR measurements. The vacuum drying setup for the polymer samples can be seen in Figure 2.1.

To prepare stock solutions of hydrotropes and derivatives (ATP, TP, AMP, adenine, and adenosine), each compound was precisely weighed and added to 10 mL volumetric flasks. For the preparation of ATP and AMP solutions, a 2 mL volumetric flask was used instead of a 10 mL one due to the limited weight of the compound. These compounds were then dissolved in deionized water (or $D_2O$ for NMR measurements) to achieve specific concentrations for the stock solutions. The desired lower concentrations were obtained through a serial dilution of the stock solutions with deionized water / $D_2O$. Once the stock solutions of ATP and its derivatives were prepared and diluted to the desired concentrations, the appropriate volumes of these diluted stock solutions were added to the previously lyophilized polymer samples (PNIPAM or PDEA). Specifically, for the LCST and ATR-FTIR measurements, 100 μL of ATP/subgroup samples were added to lyophilized polymer samples. This amount was 500 μL for the NMR measurements. Finally, the mixture of polymer and ATP samples was stored in the refrigerator overnight to ensure complete mixing.

## 2.3 Methods

### 2.3.1 Lower Critical Solution Temperature (LCST) Measurements

The phase transition measurements of 5 mg/mL PNIPAM and PDEA were performed with an OptiMelt MPA 100 instrument (Stanford Research Systems, USA), equipped with a microprocessor-controlled temperature range of 10 - 400°C. It also has a built-in camera, allowing real-time visualization of the sample during heating for observing phase transitions. The capillary tubes had 1.2-1.5 x 80 mm dimensions and were purchased from Paul Marienfeld GmbH & Co KG. The temperature was increased at a rate of 1 °C/min. In general, three, but at least 2 trials were completed for all solutions.


**Figure 2.2:** The Optimelt instrument, placed inside a refrigerator or freezer during the measurement.

The image of the Optimelt instrument can be seen in Figure 2.2. The temperature at which the polymer sample undergoes a phase change can be observed, and the point where there is a sudden change in both the phase of the sample and, consequently, the intensity of scattered light, is taken as the phase transition temperature point.

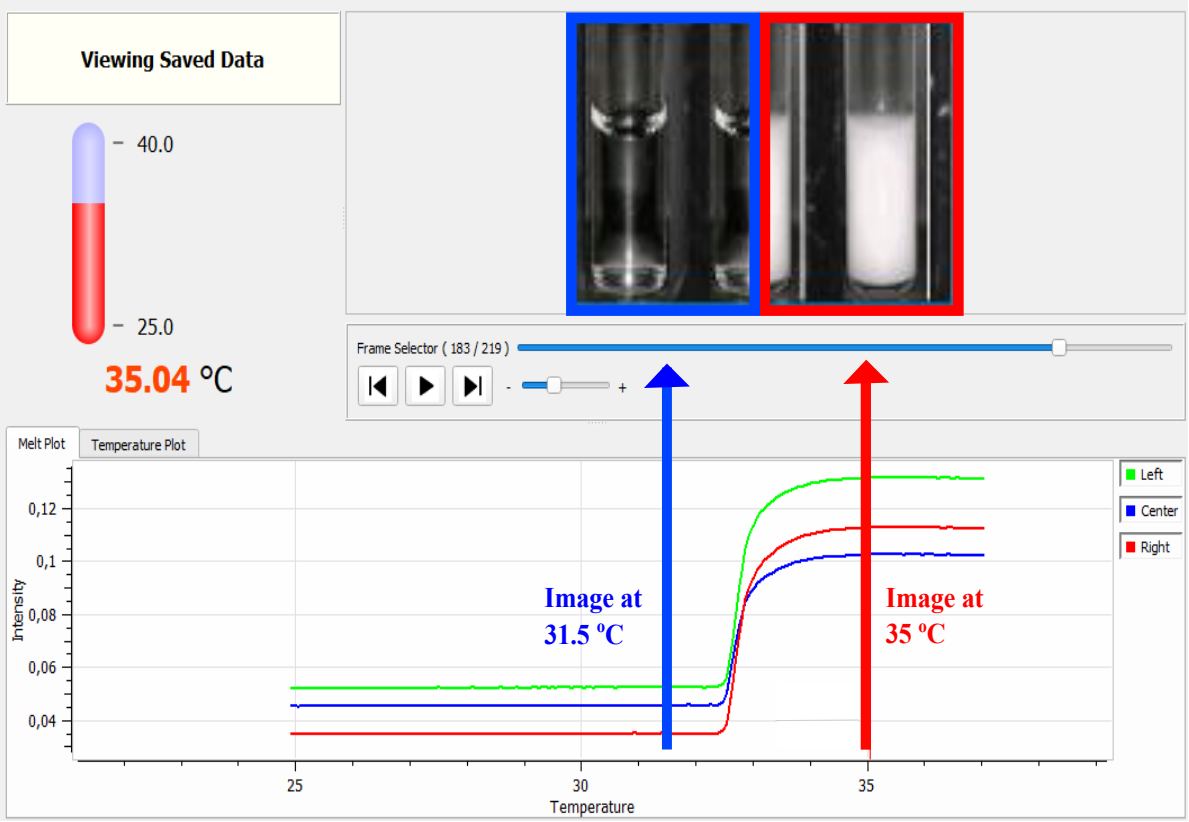


**Figure 2.3:** The Meltview window displays a plot of scattering intensity against temperature and a camera view.

For the LCST measurements, 100 µL of ATP / subgroup and polymer mixtures were carefully injected into three capillary tubes using disposable syringes (from Iso-Lab, 2 mL). For this process, ensuring an equal amount of solution in each capillary tube is crucial for accurate and precise measurements. First, the capillary tubes are filled with 10 µL of the desired solution for measurement, the Optimelt instrument is powered on, and the temperature

range is adjusted through the Optimelt software. The temperature ramp should start below the LCST of the polymers (PNIPAM and PDEA), so it is adjusted accordingly. Once the instrument is prepared, three capillary tubes are inserted into their designated positions, and the measurement begins. It is advisable to place the samples in an ice bath to prevent any turbidity formation in the sample before the measurement, especially if the phase transition of the sample mixture is close to room temperature.

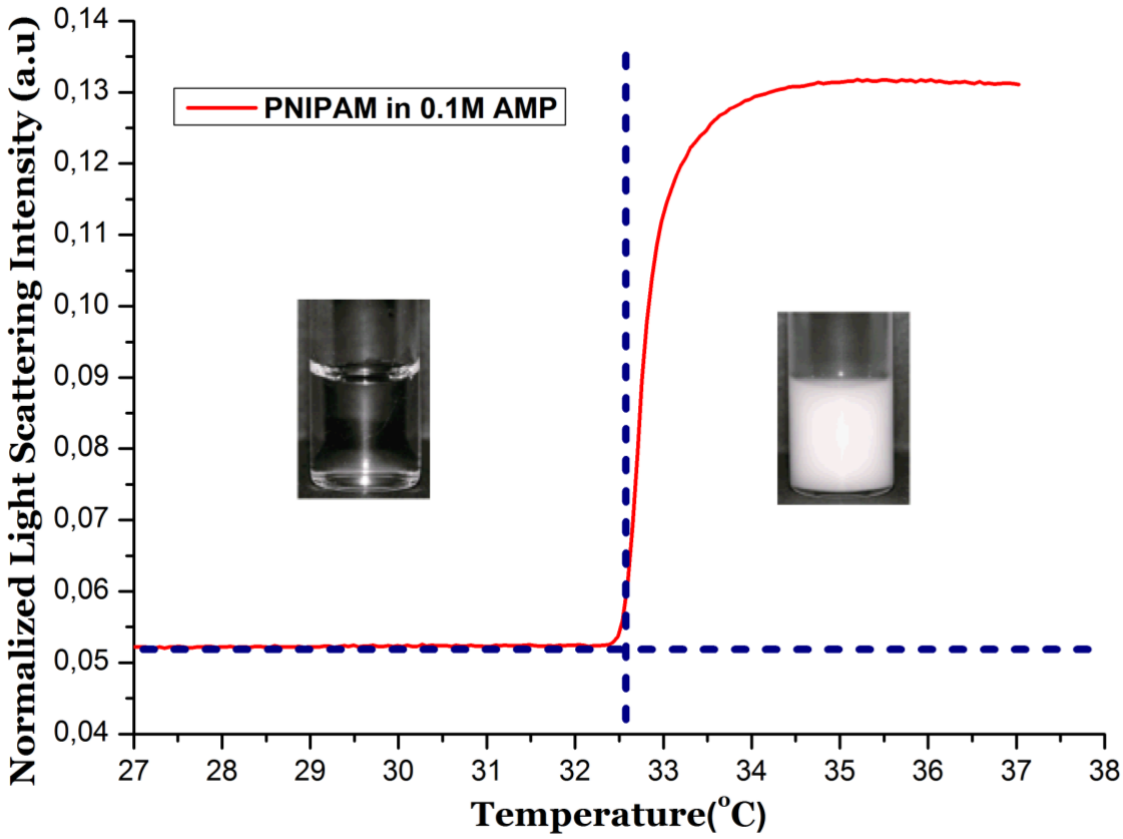


**Figure 2.4:** The graph displays the normalized scattering light intensity (a.u.) plotted against temperature (°C) for PNIPAM in 0.1M AMP. The image on the left corresponds to the unfolded (or uncollapsed) state of PNIPAM below the LCST, while the image on the right represents the folded (or collapsed) state of PNIPAM above the LCST. Dashed lines are placed on both axes of the graph to indicate the starting point of the light intensity change over the temperature range.

### 2.3.2 ATR-FTIR Spectroscopy Measurements

Attenuated Total Reflectance – Fourier Transform Infrared Spectroscopy (ATR – FTIR) measurements were utilized to probe the collapsed state of macromolecules in the presence and absence of ATP / derivative molecules. Two Bruker ALPHA II compact FT-IR spectrometers were employed that are equipped with a platinum attenuated total reflection (ATR) setup consisting of a monolithic diamond crystal tightly soldered into tungsten carbide. One of these spectrometers was equipped with an internal heating system. The other instrument lacks an internal heating system, and thus two different external heating equipment were utilized. While one of them heats the ATR crystal from the sides, the other setup helps in heating the crystal from above. After turning on the heating equipment and properly positioning it on top of the ATR crystal to achieve the desired temperature on the ATR crystal, at least a 30-minute waiting period is required for both temperature control setups. The temperature of the external heating setup was set to at least 10 °C higher than the highest LCST of samples to ensure that it adequately heats the ATR crystal to reach the desired temperature. The second spectrometer did not require any external heating device as it already could set and control the temperature within the desired range. The temperature was adjusted to 50 °C for this spectrometer.

The data acquisition for all the ATR-FTIR measurements followed specific setup parameters. The measurements were performed with 2 $cm^{-1}$ resolution, and both the sample and background scans consisted of 32 scans each. The recorded data spanned the range of 4000 $cm^{-1}$ to 400 $cm^{-1}$. Background spectra were initially recorded and followed by the acquisition of sample spectra following the experimental procedure. The samples were

analyzed in the following sequence: pure water ($H_2O$), polymer (PNIPAM or PDEA) in water ($H_2O$), ATP / derivatives in water ($H_2O$) at concentrations ranging from 0.01 to 0.5 M, and a mixture of polymer (PNIPAM and PDEA) with ATP/subgroup in water ($H_2O$). For each sample of interest, 50 μL of a 20 mg/ml macromolecule solution was transferred on top of the ATR crystal. Spectra were then captured at four specific time points: immediately after placing on top of the ATR crystal, at 3 minutes, 5 minutes, and 10 minutes. These time variation measurements were performed to ensure to capture of any time-dependent change within the collapse process. As it is discussed later in the results section the time-dependent intensity changes are minimal.

### 2.3.3 Nuclear Magnetic Resonance (NMR) Measurements

H-NMR measurements were utilized using a Bruker AVANCE III 400 MHz spectrometer. All NMR samples were measured at ambient temperature in a temperature-controlled room ($T < 21^oC$), which is kept below the phase transition temperature of PNIPAM in all studied cases. The spectra were calibrated with an external referencing with sodium 2,2-dimethyl-2-silapentane-5-sulfonate (DSS) in a $D_2O$ solution. The PNIPAM samples were placed in the outer part of the NMR tube, while the DSS solution was kept in the inner tube. Therefore, the DSS reference sample never gets in contact with the PNIPAM solutions. Data processing was carried out using the TopSpin software from Bruker and the Mestrenova software, from Spain.

### 2.3.4 Raman Spectroscopy

The continuous laser light interacts with the aqueous solution of the samples in various ways. The majority of monochromatic light that interacts with molecules scatters elastically at a frequency equal to that of the incident laser light (Rayleigh scattering). About one in $10^6$ photons are inelastically scattered, that are dispersed at a frequency that is either higher (anti-Stokes, less likely) or lower (Stokes) compared to the incident light. Raman scattering is an example of this inelastic scattering phenomenon, where the vibrational and rotational modes of the molecule are represented by the frequency differences between the incoming and scattered light. Using a Low Noise Continuous Wave (CW) Diode-Pumped Solid-State (DPSS) Laser (Ventus 532) at 532 nm at 50 mW with 10 % attenuation as the excitation laser source, the samples Raman spectra were measured with a Jobin Yvon Horiba Raman System with an Andor charge-coupled device (CCD) camera. It was employed by a < 0.01 electron/pixel/second dark current response by thermo-electrically cooling the detector to -69 $^{o}$C. The laser light is directed to the sample and collected with a 10x objective. The collected light was directed to 600 g/mm grating and finally measured by a 1024 x 256 pixel CCD camera. Unless specified otherwise, spectra were obtained using a 5-minute integration period. All the measurements were performed at ambient temperatures.

In the Raman signal of aqueous solutions, intrinsically chemical information regarding the solvent, solute, and the hydration shell of the solvent around the solute molecule is present. MCR- details: backscattered Raman light from the middle of the aqueous solution contained in a spectroscopic 1 cm glass cuvette within a thermoelectric, temperature-controlled, translating cell holder (Quantum Northwest Inc.)

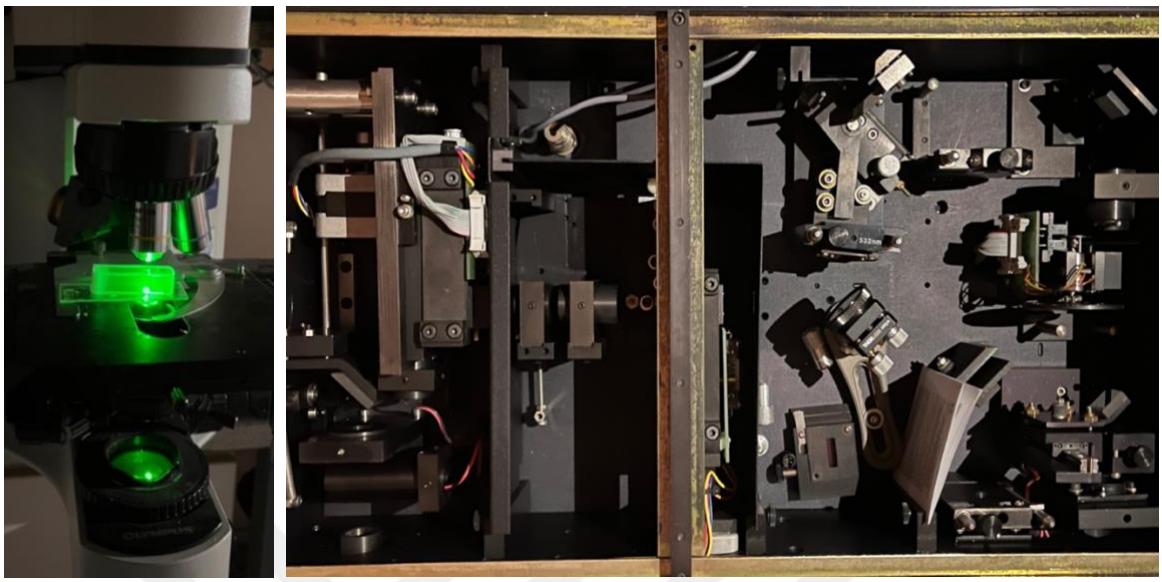

**Figure 2.5:** The setup for the Raman (MCR) process. Illumination of the Sample Cuvette by the green laser beam (left figure), and the instrument compartment (right figure).

### 2.3.5 Molecular Dynamic (MD) Simulations

The molecular dynamics (MD) simulations were carried out with GROMACS simulation package version 2021.5. The simulations of fully atomistic models of uncharged PNIPAM chains consisting of 35 monomers were performed in a cubic simulation cell which was filled with desired ATP and water molecules. The dimensions of the cubic box were 15.38 nm in each axis direction. The water model used was SPCE-E and the water molecules are models of the charmm-TIP3P interaction potential. A total of four different simulations were performed, each involving the same PNIPAM chain but varying in the ATP concentration. The concentrations of ATP investigated were 0.1M, 0.2M, 0.3 M, and ATP-free solutions. The charge of ATP is neutralized by the addition of $Na^+$ ions, which is parametrized using the Charmm36 force field. The system underwent energy minimization using the steepest-descent algorithm before the actual Molecular Dynamics (MD) simulation. This MD simulation lasted for 250 ns and was conducted in an NPT ensemble at a temperature of 310 K, which is above

the Lower Critical Solution Temperature (LCST) of PNIPAM in pure water. In the simulations, the temperature was controlled using a velocity-rescaling thermostat with a time constant of 0.1 ps, while the pressure was maintained at an equilibrium value of 1 bar using a Parrinello-Rahman barostat with a time constant of 2.0 ps. To enhance statistical robustness, each simulation was replicated 2 times. Periodic boundary conditions are applied in all three dimensions. Time propagation is accomplished using a leapfrog integrator with a time step of 2 fs. For van der Waals and Coulomb interactions, a cutoff of 1.2 nm is utilized. Long-range electrostatic interactions are treated using the particle-mesh Ewald (PME) method with a grid spacing of 0.16 nm. The LINCS32 algorithm is used to constrain the bonds involving hydrogen atoms and the bonds and angles of the water molecules. For energy and pressure, long-range dispersion corrections have been used. The trajectories obtained for all systems were analyzed using Visual Molecular Dynamics (VMD).

# Chapter 3 – Results and Discussion

## 3.1 Phase Transition Temperatures of Macromolecules as a Function of ATP (or subgroups) Concentration

The presence of hydrotropes influences the phase transition temperature of biomacromolecules. With the characteristic nature of destabilizing the formation of macromolecular aggregates in aqueous solution, one would expect an increase in the phase transition temperature of thermoresponsive macromolecules.

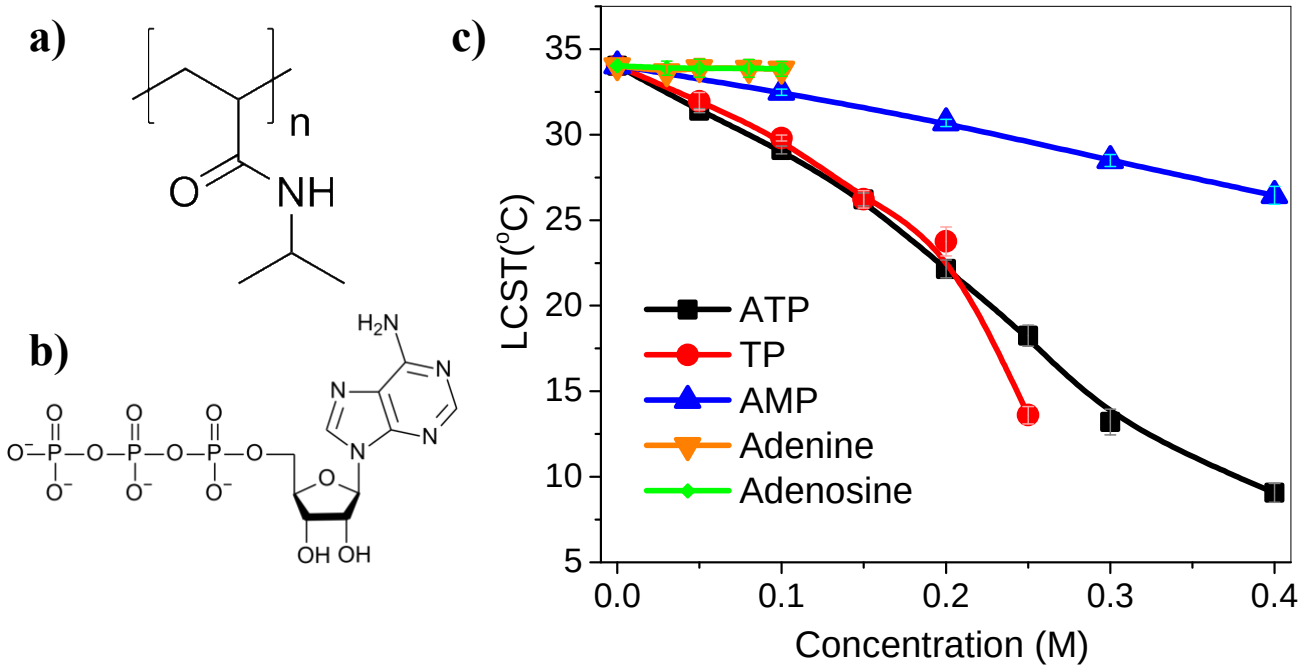


**Figure 3.1: a)** The structure of Poly (N – isopropyl acrylamide) (PNIPAM). **b)** The structure of ATP molecule. **c)** The LCST of 5 mg/mL PNIPAM as a function of ATP, TP, AMP, Adenine, and Adenosine concentrations(M). Error bars indicate the standard deviation of data. The solid lines are a guide to the eye.

Figure 3.1 shows the LCST measurements of 5 mg/ml PNIPAM solutions as a function of ATP, TP, AMP, adenine, and adenosine concentrations. First, the LCST of

PNIPAM in the absence of any hydrotrope is at 34.22 ºC. The LCST values of PNIPAM in the presence of both adenine and adenosine (green rhombus and orange triangles) remained nearly unchanged, indicating that these relatively hydrophobic groups of ATP do not have a significant effect on the aggregation temperature of PNIPAM. The measurements for adenine and adenosine were restricted up to 0.1 M due to the limited solubility. Note that, these concentrations still substantially exceed the typical physiological levels.

In contrast, the LCST values of PNIPAM solutions exhibited a decreasing trend as a function of ATP concentration (black squares). This trend indicates a strong "salting-out" behavior. Such salting-out behavior of ATP contrasts with its anticipated hydrotropic behavior, which typically involves enhancing or not influencing the solubility of macromolecules. Similarly, the presence of the triphosphate (TP) and adenosine monophosphate (AMP) groups also induced a comparable salting-out behavior in the phase transition temperature of PNIPAM. However, while both ATP and TP resulted in a substantial monotonic decrease in the LCST of PNIPAM, a shallower decrease was observed in the presence of AMP. It indicates that the triphosphate group should mainly cause the salting-out behavior. To further explore the role of ATP as a hydrotrope, the same procedure was executed using another model macromolecule Poly (*N*, *N*- diethyl acrylamide), referred to as PDEA, which possesses a similar structure to PNIPAM. The structure of PDEA is depicted in the inset of Figure 3.2. The LCST behavior of PDEA as a function of the tested hydrotropes was similar to the PNIPAM ones (Figure 3.2). Namely, the LCST of PNIPAM was influenced marginally in the presence of adenine and adenosine, whereas monotonically decreased with increasing ATP and TP concentrations. The subsequent section will provide detailed information on the LCST measurements of PDEA.

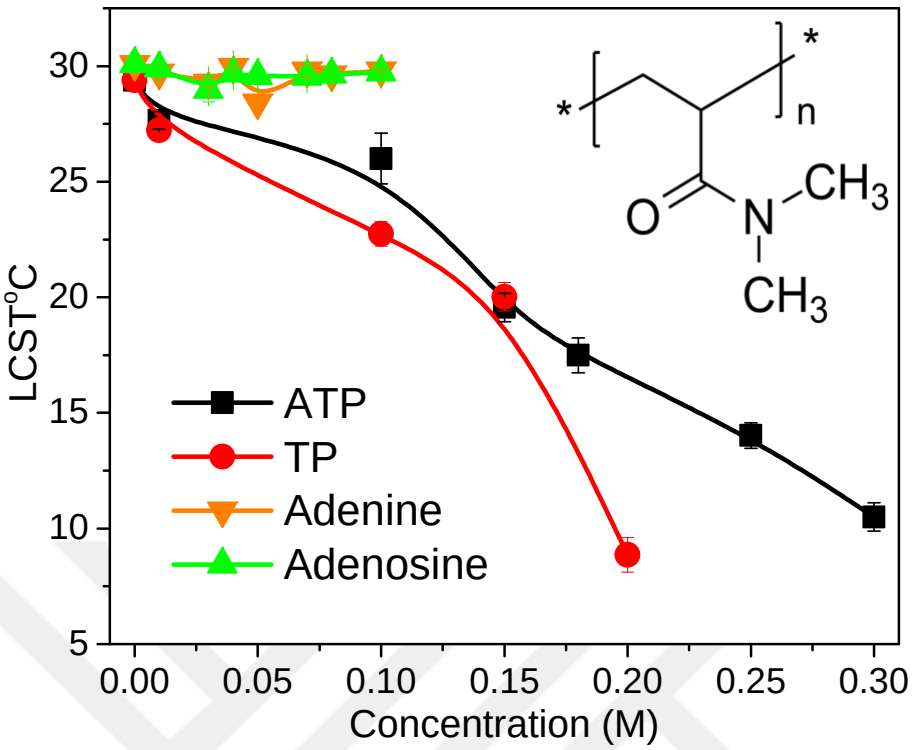


**Figure 3.2:** The LCST of 5 mg/mL PDEA as a function of ATP, TP, Adenine, and Adenosine concentrations(M). Error bars indicate the standard deviation of data for many data points, it is within the data points drawn. The solid lines are a guide to the eye. Inset shows the structure of poly (*N*, *N*- diethyl acrylamide) (PDEA).

### 3.1.1 Investigation of Charge on the Phase Temperature of Macromolecules

The phase transition temperature of macromolecules can be influenced by the pH of the solution. Moreover, the phosphate ATP can also change its charge state as the pH of the solution alters. In order to make sure the protonation and deprotonation are not influencing the trends in the phase transition of macromolecules, a different PDEA macromolecule was also employed. The charged PDEA has only 2 deprotonated carboxylate groups at the C and N termini of the polymer. The LCST in the absence and presence of buffer shows around 3 °C. In the presence of 0.1 M tris buffer at pH 7.74, and an uncontrolled pH solution, the LCST

trends as a function of ATP and TP, were found to be quite similar to one another. Moreover, the LCST trends are similar to those of neutral PDEA (see Figure 3.3).

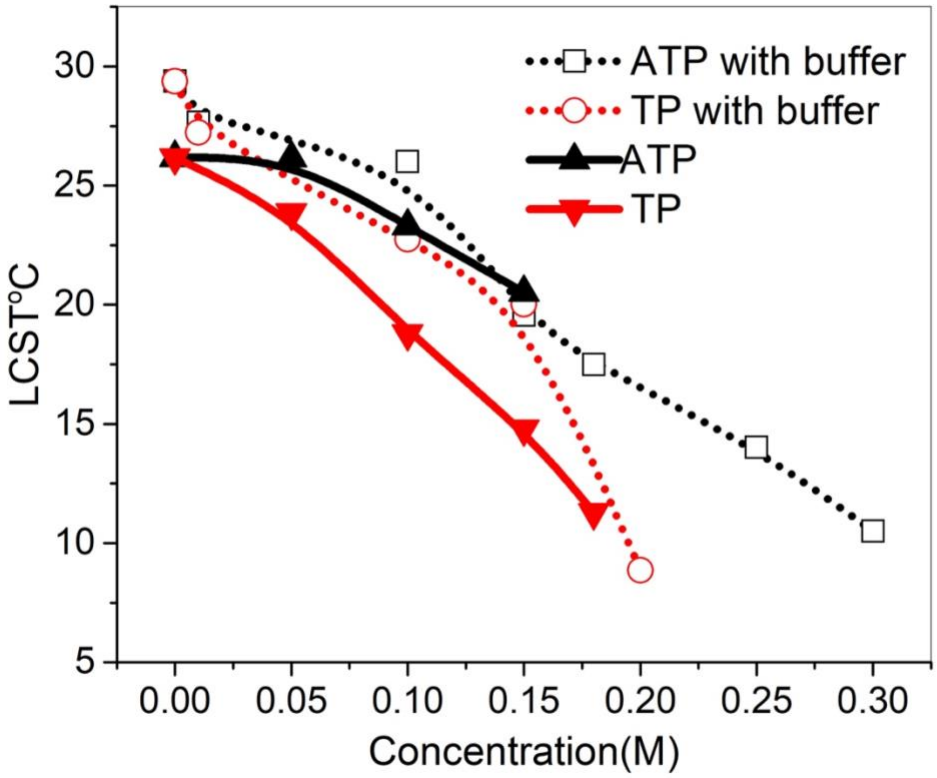


**Figure 3.3:** The lower critical solution temperature (LCST) of 5 mg/mL charged PDEA is plotted as a function of ATP (black) and TP (red) concentrations (M). The solid lines represent the LCST of charged PDEA without any buffer, while the dashed lines represent the LCST of the same charged PDEA in the presence of 0.1M Tris Buffer. Both the solid and dashed lines serve as a guide to the eye.

When the charged PDEA was employed in the LCST measurements of adenine and adenosine, some relative changes were observed. Figure 3.4 illustrates the LCST results for both charged and neutral PDEA in the presence of adenine (orange) and adenosine (green). LCST measurements with neutral PDEA revealed minimal alteration in the lower critical solution temperature of PDEA. In contrast, using charged PDEA resulted in some measurable

decrease in the relative LCST values with the LCST in water. To explore potential charge and pH-related factors in this scenario, the solutions were prepared in 0.1 M tris buffer at pH 7.74, When the buffer was present in the solutions, there was a reduced change in the LCST (Figure 3.4b). Consequently, under these conditions, the obtained results closely mirrored those observed with neutral PDEA.

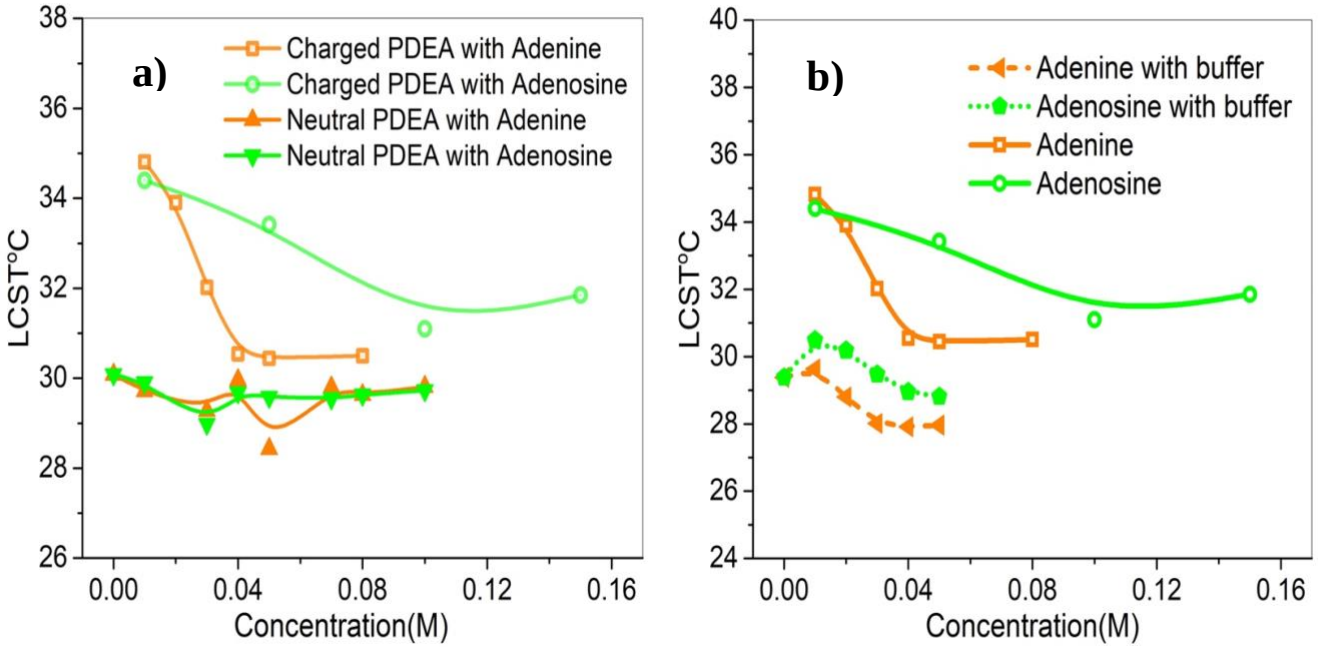


**Figure 3.4:** The lower critical solution temperature (LCST) of 5 mg/mL charged PDEA is plotted as a function of adenine (orange) and adenosine (green) concentrations (M). **a)** The solid lines depict the LCST of charged PDEA without any buffer, while the transparent lines represent the LCST of neutral PDEA without any buffer. **b)** The solid lines continue to represent the LCST of charged PDEA without any buffer (as in part a), while the dashed lines indicate the LCST of the same charged PDEA in the presence of 0.1M Tris Buffer. Both the solid and dashed lines are provided as a guide to the eye.

### 3.1.2 The Effects of Cations on the Phase Temperature of Macromolecules

In the next set of experiments, the impact of the presence of physiologically relevant cations on the phase transition of macromolecules was investigated. The presence of $Mg^{2+}$ ions was proposed to be a key ingredient for its hydrotropic action. [122] To test the influence of $Mg^{2+}$ cations, 10 mM of $MgCl_2$ and 10 mM of NaCl salts were added to different ATP solutions, and the LCST values of PNIPAM were measured as a function of ATP concentration. As can be seen from Figure 3.5, the phase transition temperature of PNIPAM is not influenced by the presence of additional chloride salts of the cations. This indicates that the observed unexpected salting-out behavior of ATP on the phase behavior of PNIPAM is in fact real.

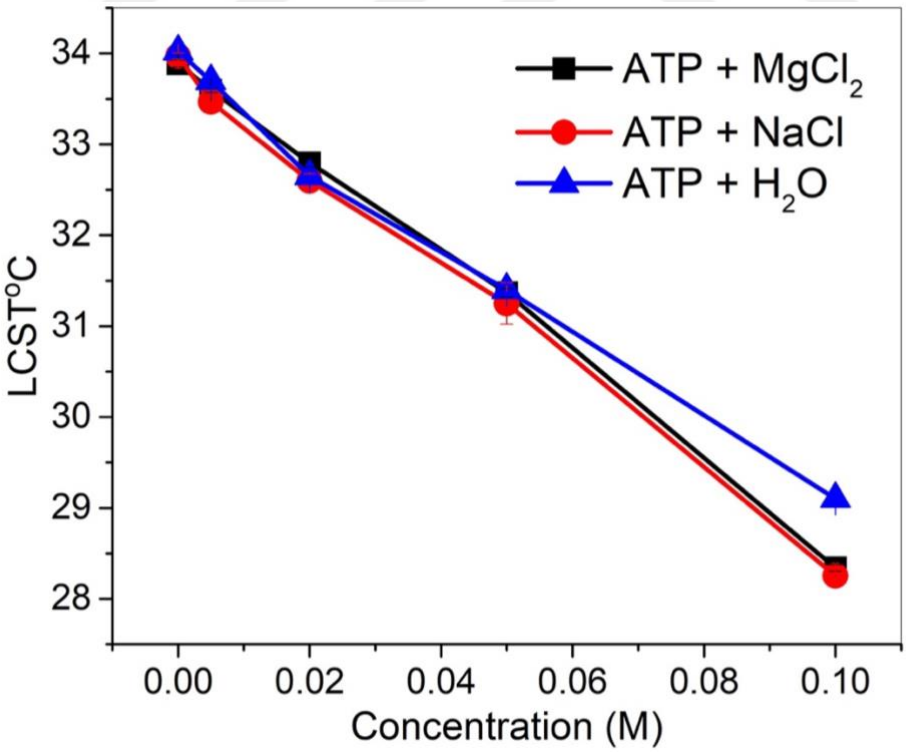


**Figure 3.5:** The LCST of 5 mg/mL PNIPAM in the presence of ATP in $MgCl_2$, ATP in NaCl, and ATP in aqueous solutions, as a function of ATP concentrations (M). Error bars indicate the standard deviation of data. The solid lines are a guide to the eye.

### 3.1.3 Phase Transition Temperatures of a Classical Hydrotrope

The substances commonly linked with the term "hydrotrope" are primarily the sodium salts of short alkylbenzene sulfonates. [119] In these compounds, the anion is amphiphilic and bulky, with amphiphilicity that is not as pronounced as in typical surfactants, although they may foam considerably. [119] Another category includes water-soluble mono ethers of ethylene glycols or higher polyols. Depending on the length of the alkyl chain, they can function as "simple" co-solvents, hydrotropes, or genuine surfactants. [119] Among these, sodium xylene sulfonate (NaXS) is the most commonly utilized hydrotrope molecule. In the literature, the hydrotropic behavior of ATP is mostly compared to NaXS to highlight its efficiency being a hydrotrope. For example, Patel et. al [122] demonstrated that adenosine triphosphate (ATP) can prevent protein aggregation approximately an order of magnitude more effectively than sodium xylene sulfonate in a classic hydrotrope assay. Moreover, Mondal et al. [161] demonstrated the superior effectiveness of ATP compared to the NaXS and proposed that the crucial factor lies in ATP’s inherent capacity for self-assembly.

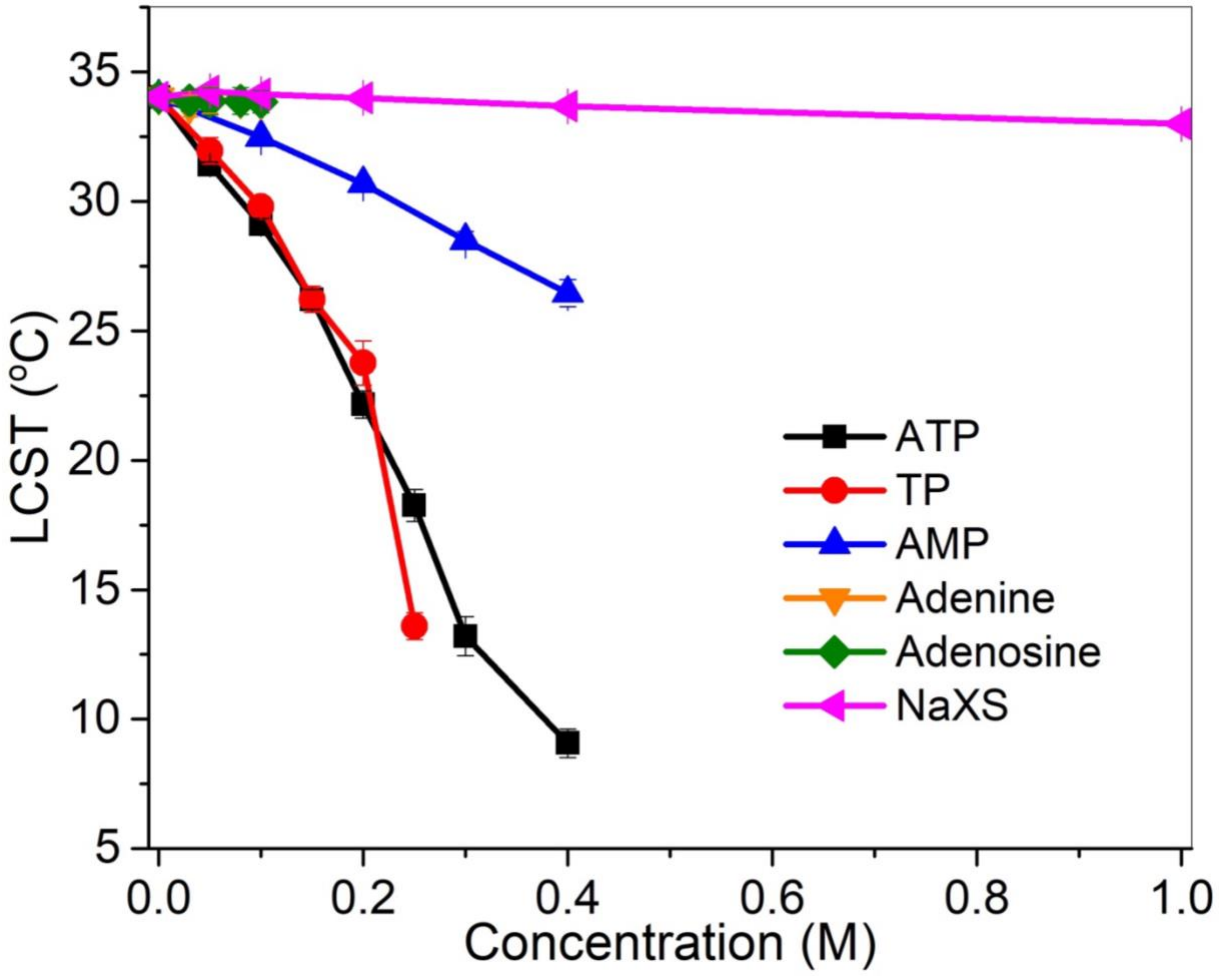


**Figure 3.6:** The LCST of 5 mg/mL PNIPAM as a function of ATP, TP, AMP, adenine, adenosine, and NaXS concentrations (M). Error bars indicate the standard deviation of data. The solid lines are a guide to the eye. The inset shows the structure of sodium xylene sulfonate (NaXS).

Here, LCST measurements of PNIPAM were conducted in the presence of a well-known chemical hydrotrope, NaXS, the structure of which can be seen in the inset of Figure 3.6. For a comprehensive comparison of the effects on the LCST of PNIPAM, all the results of LCST measurements in ATP, TP, and AMP solutions were plotted together with the NaXS, and both sets of data are illustrated in a unified Figure 3.6. As depicted in Figure 3.6, ATP, TP, and AMP exhibit salting-out behavior on the LCST of PNIPAM, while the chemical hydrotrope NaXS follows a linear trend similar to adenine and adenosine and does not demonstrate any salting-out behavior on PNIPAM. Such results along with the literature data

demonstrate the influence of ATP on macromolecules is beyond the general behavior of hydrotropes. In order to explore the molecular mechanisms of the influence of ATP on neutral macromolecules with random-coil-like structures, spectroscopic measurements were performed.

## 3.2 ATR-FTIR Measurements: Investigation of the Collapsed States of Macromolecules as a Function of ATP (or subgroups) Concentration

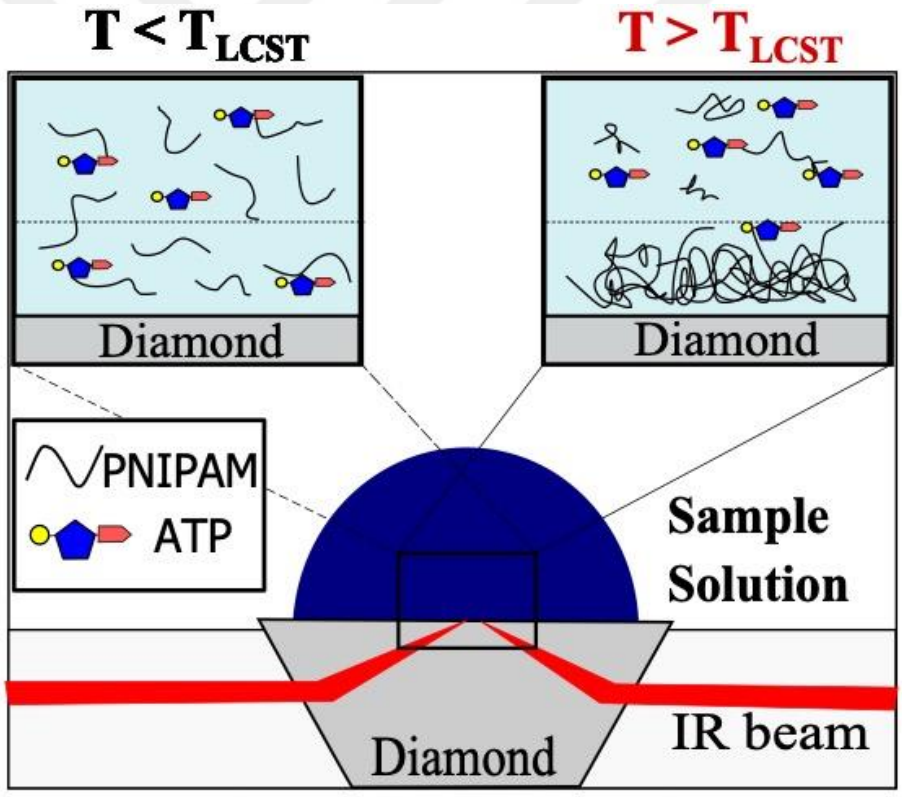


**Figure 3.7:** The illustration of the PNIPAM in ATP solution droplet below and above the LCST.

ATP molecule and its subgroups, in sharp contrast to general hydrotropic behavior, demonstrate an apparent salting-out influence on the PNIPAM macromolecule. To gain a molecular-level understanding of this effect in aqueous environments, the macromolecule above its phase transition temperature is investigated via ATR-FTIR spectroscopy. Specifically, we investigated the collapsed state of the PNIPAM macromolecule with and without the presence of ATP and its derivative in the macromolecule solutions. Figure 3.7 depicts the ATR-FTIR working principle illustrating the macromolecule solution droplet, with the upper left box showing the measurements below the LCST and the right box showing measurements above the LCST. As can be seen, if the temperature is low (below LCST), no PNIPAM phase separation is formed on the ATR diamond. However, at high temperatures (above LCST), PNIPAM molecules are collapsed onto the crystal, allowing us to observe and investigate the collapse state of PNIPAM, and the salt ions via absorbances of vibrational bands of the molecules, which can be exemplified in Figure 3.9.

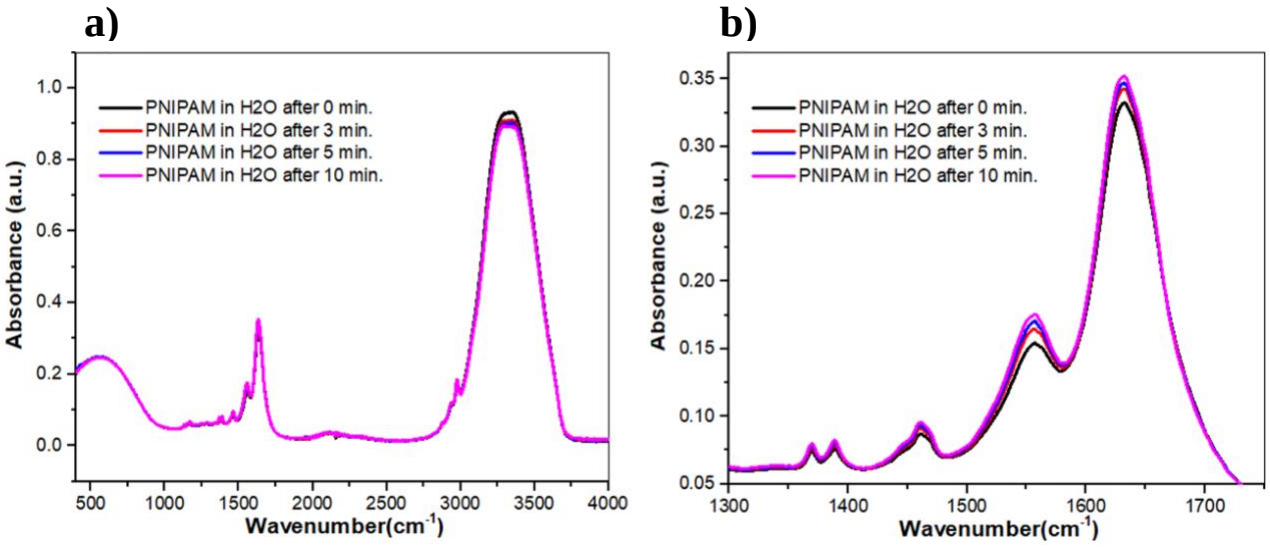


**Figure 3.8:** a) The ATR – FTIR spectra of the 50 µL of PNIPAM in $H_2O$, measured after 0, 3 , 5, and 10 min., at 50 °C. b) The same spectrum as in part a, focusing on the 1310 – 1750 $cm^{-1}$ region. The arrows represent the inclines and declines in PNIPAM's aggregation.

The phase separation of macromolecules is a kinetic process. To make sure the phase separation process is over, the ATR-FTIR spectra are measured at different times, Thus, in the first set of ATR-FTIR measurements, the aim was to investigate the kinetics of the phase change of PNIPAM macromolecules in aqueous conditions. To investigate this parameter, ATR-FTIR spectra of PNIPAM in sole water at 50 °C were recorded at four different time intervals after the macromolecule solution was introduced on top of ATR equipment. The overall spectra for PNIPAM are shown in Figure 3.8 at 0 min., 3 min., 5 min., and 10 min., respectively. In Figure 3.8, a slight variation in PNIPAM's aggregation (1500-1600 $cm^{-1}$) is evident. Despite this, the increase in PNIPAM aggregation being only 5% over 10 minutes suggests that the time duration exerts minimal influence on the overcome. This conclusion is reinforced by the results shown in this subsection, where the average standard deviation in the ratio of PNIPAM in the ATP/derivative solution to PNIPAM in water is approximately ± 30%. To ensure data compatibility and maintain consistent parameters, all further spectra shown in the thesis were the ones recorded at 3 minutes. Note that, the conclusions drawn in this subsection do not change even other sets of data recorded at different times were utilized instead. Figure 3.9 shows the ATR-FTIR measurements of PNIPAM in the presence of 0 M, 0.05 M, and 0.2 M of aqueous ATP at 50°C (above the LCST).

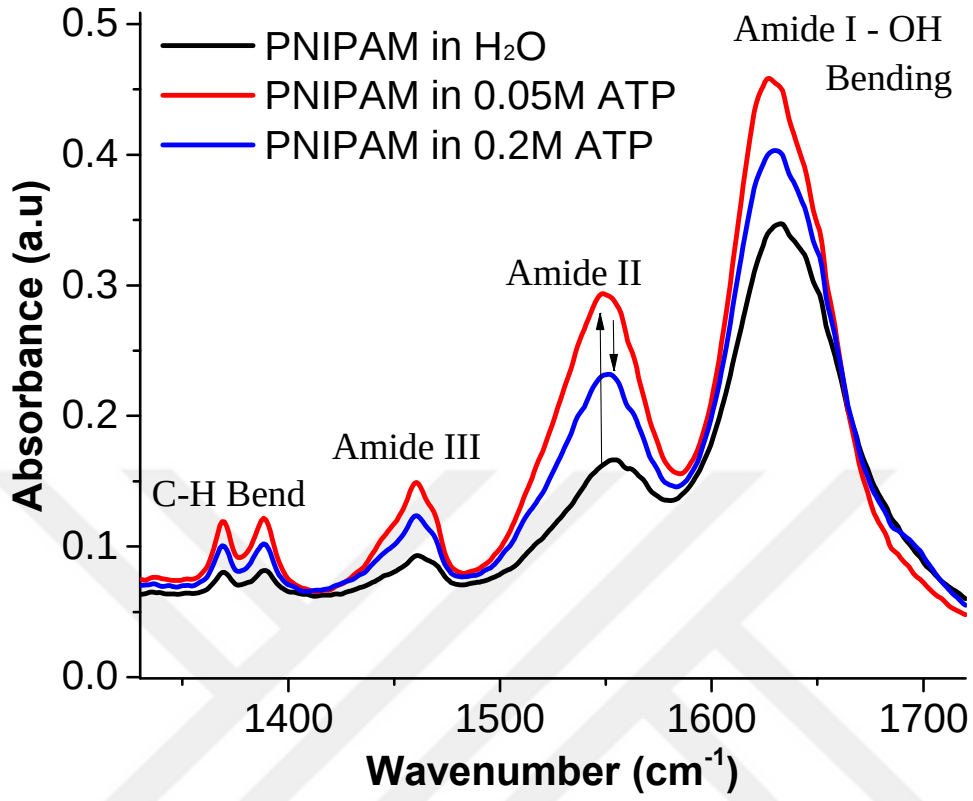


**Figure 3.9:** ATR-FTIR spectrum of 20 mg/mL PNIPAM in the presence of water (black), 0.05M ATP (red), and 0.2M ATP (blue).

The observation of characteristic absorption bands (Amide I (1625 $cm^{-1}$), Amide II (1545 $cm^{-1}$), Amide III (1470 $cm^{-1}$), and CH bands (1355-1409 $cm^{-1}$) indicates the collapsed aggregates are present on the ATR crystal. In Figure 3.9, there is a notable increase in the intensity of PNIPAM peaks in the presence of 0.05M ATP in contrast to sole water (0 M ATP), particularly in the Amide II (1545 $cm^{-1}$) region. The increment of PNIPAM-related bands in the presence of ATP supports the salting-out effect exhibited by ATP in the LCST measurements. However, as the concentration of ATP further increased to 0.2 M a less effective salting-out effect is observed. While this surprising observation of PNIPAM aggregation persists beyond the concentration range of approximately 0.15 M, still signifying a salting-out effect, it is clear that there is an underlying phenomenon at play here.

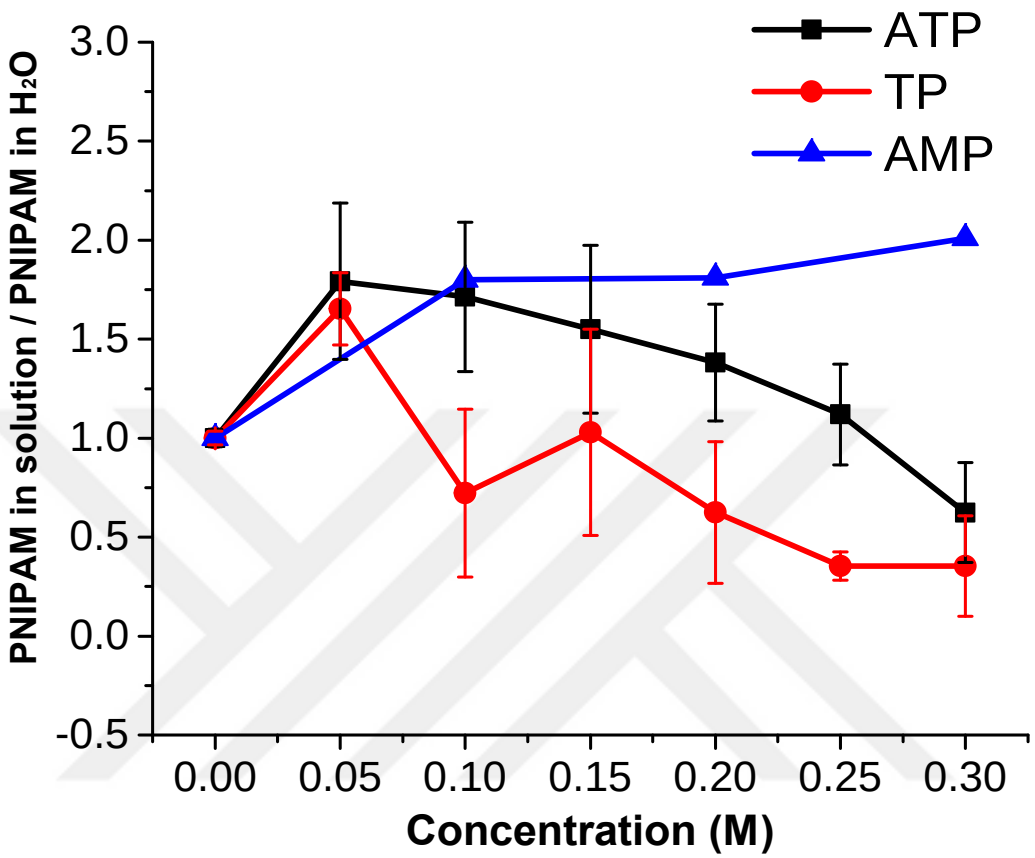


**Figure 3.10:** The ratio of PNIPAM in ATP, TP, and AMP solutions to PNIPAM in water as a function of ATP/derivative concentration.

Figure 3.10 illustrates the ratio of amide II bands (at 1545 $cm^{-1}$) of PNIPAM aggregation in ATP solutions to its aggregation in aqueous solution as a function of ATP concentrations. The ratio equals one when PNIPAM aggregation in ATP solution is the same as in $H_2O$, as depicted with the gray dashed line. As can be seen, once the ratio peaks at 0.05 M of ATP, corresponding to the highest level of PNIPAM aggregation, it subsequently begins to decrease, indicating that at higher ATP concentration, there are lesser amounts of PNIPAM aggregates compared to the solution of PNIPAM in sole $H_2O$. At high enough concentrations of PNIPAM, the value gets below unity. A similar trend can be observed in the PNIPAM ratio

for TP solution to sole water. Yet the ratio gets down to approximately unity around 0.1 M ATP concentration. In contrast to the intensity ratio of PNIPAM in both ATP and TP, the aggregation ratio of PNIPAM monotonically increased without any subsequent decrease in the presence of AMP. This observation suggests although the salting-out is formed for all 3 molecules (ATP, TP, and AMP) the underlying phenomenon can be quite different.

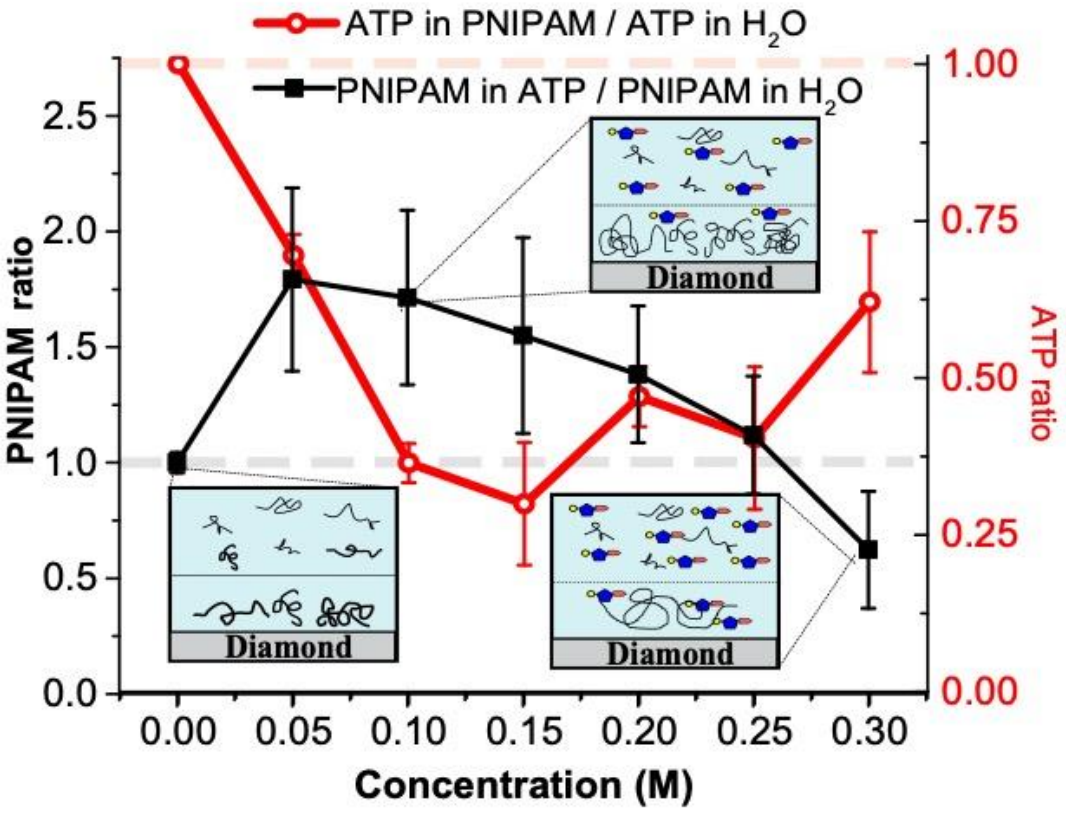


**Figure 3.11:** *(left y-axis, black)* The ratio of PNIPAM in ATP with respect to PNIPAM in water as a function of ATP/derivative concentration. *(right y-axis, red)* The ratio of ATP peaks in the PNIPAM solution to the one in sole water.

In addition to exploring the collapsed state of the macromolecule, the role of ATP on the macromolecule aggregation was also explored. To examine the behavior of ATP in collapsed PNIPAM, the peak ratio at ~1071 $cm^{-1}$ (P-O stretching band) of different

concentrations of ATP solutions in PNIPAM to pure water was monitored. The ratio of ATP is shown in Figure 3.11 (red empty circles) together with the ratio of PNIPAM in ATP/$H_2O$ solutions (black squares) as a function of ATP concentrations. This methodology was previously employed to elucidate the role of guanidium salts on the collapsed state of ELPs.[162] As previously discussed, in Figure 3.11 the ratio of PNIPAM in the presence of ATP compared to the one in sole $H_2O$ (depicted as black squares) starts to decrease after reaching a maximum at an ATP concentration of 0.05M. In contrast, the ATP ratio decreases up to 0.1 - 0.15 M, after which it begins to increase again. This data suggests a mechanistic view of the macromolecular collapse, ATP remains mainly excluded from the macromolecular aggregation. The small illustrations in Figure 3.11 show the aggregation levels of PNIPAM and ATP molecules at different ATP concentrations. This phenomenon can be described as similar to the excluded volume effect which was introduced by Werner Kuhn in 1934. Paul Flory soon applied this concept to the polymer molecules. This phenomenon of excluded volume leads to the emergence of depletion forces. In the realm of polymer science, excluded volume refers to the notion that a segment of an elongated chain molecule cannot occupy a space already taken up by another segment of the same molecule. [163] Overall, both the LCST and ATR-FTIR measurements indicate the presence of salting-out mechanisms exclusively, without any indication of interaction between the macromolecule and ATP. In the next section to offer site-specific information about any interaction between the macromolecules and ATP and its derivatives by observing the H-base residual, $^1$H-NMR titrations of PNIPAM were conducted in heavy water solutions of ATP, TP, and AMP. The details are discussed in the following section.

## 3.3 $^{1}$H-NMR Measurements: Investigation of Site-Specific Evidence of ATP-Macromolecule Interactions

$^{1}$H- NMR has recently been employed to decipher any binding interactions between small molecules/ions and macromolecules.[104] Figure 3.12 illustrates the $^{1}$H-NMR spectrum of 5 mg/ml PNIPAM in neat $D_2O$, externally referenced to DSS in $D_2O$. The measurement procedure was described in section 2.3.3. First, note that the DSS reference molecule is responsible for four of the resonances that are visible in the spectrum. The structure of the DSS molecule is shown in Figure 3.12, located above the PNIPAM structure.

The set of nine terminal -$CH_3$ hydrogens on the Si atom is represented by the sharp and singlet reference peak at 0 ppm. DSS produces three extra multiplet signals which are marked on the spectrum as 1,2, and 3, aligning with the three methylene positions in the backbone. The multiplet with the highest chemical shift, marked with 3 at ~2.90 ppm, is associated with the methylene nearest to the sulfonate end-group. The peak's elevated chemical shift is a result of its electron-withdrawing attributes, leading to an inductive deshielding effect. The multiplet number 2 is positioned at a lower chemical shift (~1.75 ppm) owing to its greater distance from the sulfonate group. Meanwhile, the multiplet number 1 exhibits an even lower chemical shift (~0.620 ppm) as it is situated farthest from the sulfonate and closest to the Si atom, introducing a slight shielding effect attributable to its lower electronegativity.

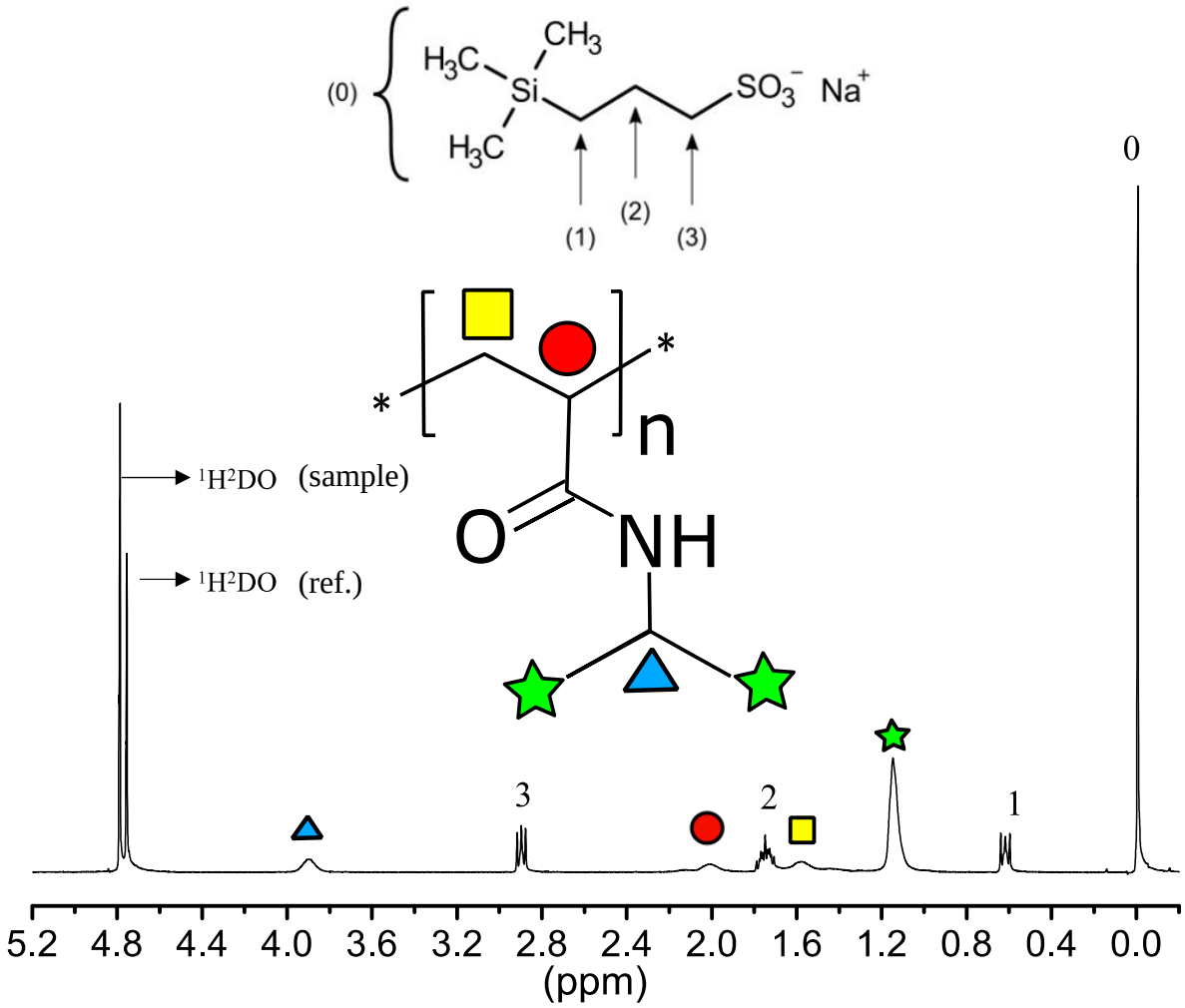


**Figure 3.12:** A representative 1H-NMR spectrum for PNIPAM in pure $D_2O$ with external referencing to DSS. The top section displays the structure of DSS, with numbered sets of H's corresponding to the four resonances labeled in the spectrum. The bottom section includes the structure of PNIPAM with color-coded annotations representing its four signals. The two water peaks (HDO in the sample and HDO in the reference solution) are also marked on the spectrum.

Apart from the DSS peaks, there are two relatively large, broad singlet-like peaks appearing at ~4.8 ppm. These peaks result from the slight presence of exchangeable hydrogen (protium, 1H) contamination in the deuterated solution environment. This contamination is commonly found at a minimal level in all deuterated protic solvents or is gradually acquired from the air or surface contacts during the process of sample preparation. In this measurement, the polymer itself emerges as a notable source of $^1H$ contamination, attributed to the presence

of the protic amide -NH moiety. Upon dissolving in $D_2O$, these exchangeable hydrogen atoms swiftly disperse within the solution.

The pure $D_2O$ water (HDO) peak is visible at 4.8 ppm. However, the presence of solutes alters the chemical and magnetic environment of the solvent molecules, resulting in observable shifts in the water peak. In the PNIPAM/neat $D_2O$ spectrum shown in Figure 3.12, the HDO peak for the sample is around ~4.78 ppm. Notably, in samples containing salt, the water peak is generally shifted further (towards lower chemical shifts), as will be demonstrated later. The HDO peak in the reference solution remains constant (unless the solution concentration is altered) and is consistently observed at approximately ~4.75 ppm.

The four major chemical shifts (color-coded) on the spectrum (Figure 3.12) correspond to distinct protons of the PNIPAM macromolecule, identified with red circle, yellow square, green star, and blue triangle. The lowest chemical shift signal, denoted with a green start is positioned at ~1.15 ppm, corresponding to the six i-Pr terminal methyl hydrogens. The following chemical shift, indicated by a yellow square at approximately 1.58 ppm, corresponds to the backbone methylene ($-CH_2$) group, which is positioned relatively far from the electronegative groups. The -CH backbone proton, alpha to the amide carbonyl (indicated with a red circle), is positioned at around 2.02 ppm because it is relatively closer to the electron-withdrawing carbonyl group. Lastly, the highest chemical shift signal of PNIPAM belongs to the CH group bonded to the amide N-atom (blue triangle) and appears at approximately 3.90 ppm.

The chemical shifts of PNIPAM were monitored as a function of ATP, TP, and AMP concentration. The overall results from $^1H$- NMR measurements are shown in Figure 3.13, where the change in chemical shift ($\delta\Delta$ ppm) for each proton signal is plotted as a function of

ATP, AMP, and TP concentration. The positions of the protons are labeled using the same color coding as in Figure 3.12. All the chemical shift changes at specific sites of PNIPAM in the presence of ATP, AMP, and TP exhibit completely linear and monotonic decreasing trends. This outcome indicates that there is no direct binding interaction between the macromolecule and any of the tested hydrotropes i.e. ATP, AMP, and TP. These results are also in line with the results shown in previous parts.

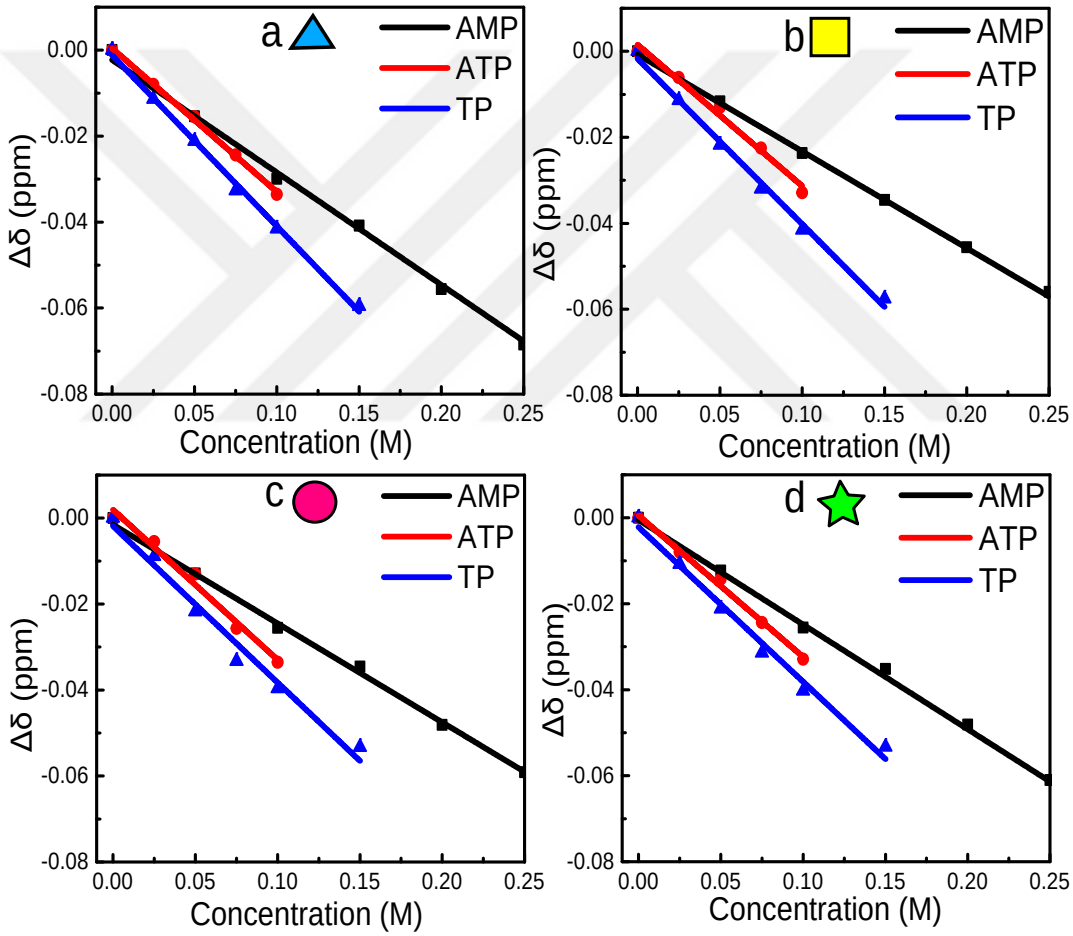


**Figure 3.13:** a-d) The four panels below illustrate the changes in the chemical shifts of each specific site as a function of the concentration of ATP, AMP, and TP. a) (blue) the N-CH group b) (yellow) the backbone CH group (alpha position to carbonyl group) c) (red) the backbone $CH_2$ group d) (green) i-Pr terminal $CH_3$ groups.

## 3.4 Molecular Dynamic (MD) Simulations

All the experimental results up to this point draw a unified mechanism. Namely, the LCST measurements indicated the salting-out effect of ATP, TP, and AMP on neutral random coil-like structured macromolecules, i.e. PNIPAM. This observation is further supported by ATR-FTIR measurements at the low (physiologically relevant) concentrations of ATP and TP molecules. Intriguingly, at elevated concentrations of ATP and its derivatives, the salting-out effect diminishes without a clear underlying cause. Notably, these measurements also reveal the exclusion of ATP molecules from the collapsed macromolecule. Additionally, proton signals' chemical shift differences in NMR measurements suggest the absence of direct binding interactions between ATP/derivatives and any chemical sites on the model macromolecules. The collective findings from these experiments suggest that ATP does not function as a hydrotrope; instead, it serves as a stabilizer for neutral amide-based macromolecules with random-coil-like structures.

To provide additional insight beyond the experimental findings discussed thus far, we conducted molecular dynamics (MD) simulations at four distinct ATP concentrations. This computational approach aims to further investigate and visualize ATP - macromolecule interactions and elucidate the underlying reasons for the observed partial reduction in PNIPAM solubility at elevated ATP concentrations during ATR-FTIR measurements. Figure 3.14 shows the first simulation of the PNIPAM polymer in the absence of ATP in an aqueous simulation medium.

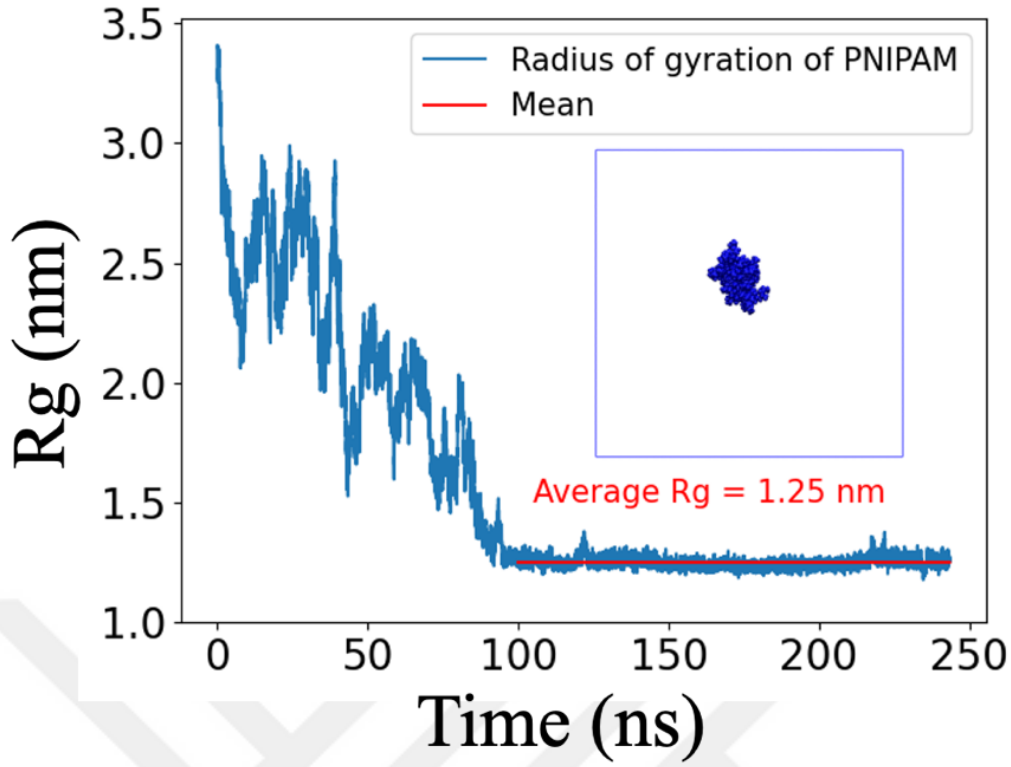


**Figure 3.14:** The radius of gyration values of the PNIPAM polymer, taken from the 250 ns simulation in free-ATP solution.

The simulations of fully atomistic models of uncharged isotactic PNIPAM chains consisting of 35 monomers were performed in a cubic simulation cell, 15.38 nm in each direction. The PNIPAM chain was initially positioned at the center of the simulation box and was unrestrained. The simulation ran for 250 ns and was conducted in an NPT ensemble at a temperature of 310 K, which is above the phase transition temperature (LCST) of PNIPAM in pure water. The simulation box was filled with water molecules, and the SPCE-E water model was used. Figure 3.14 illustrates the radius of gyration change of PNIPAM as a function of simulation time. The box inside the figure is a snapshot from the simulation, captured at 150 ns. As evident in the figure, it took approximately 100 ns to converge the system to the collapse of the macromolecule. The average radius of gyration of PNIPAM between 100-250 ns was 1.25 nm. In subsequent simulations, ATP molecules were added to the simulation boxes at concentrations matching the experimental studies of ATP.

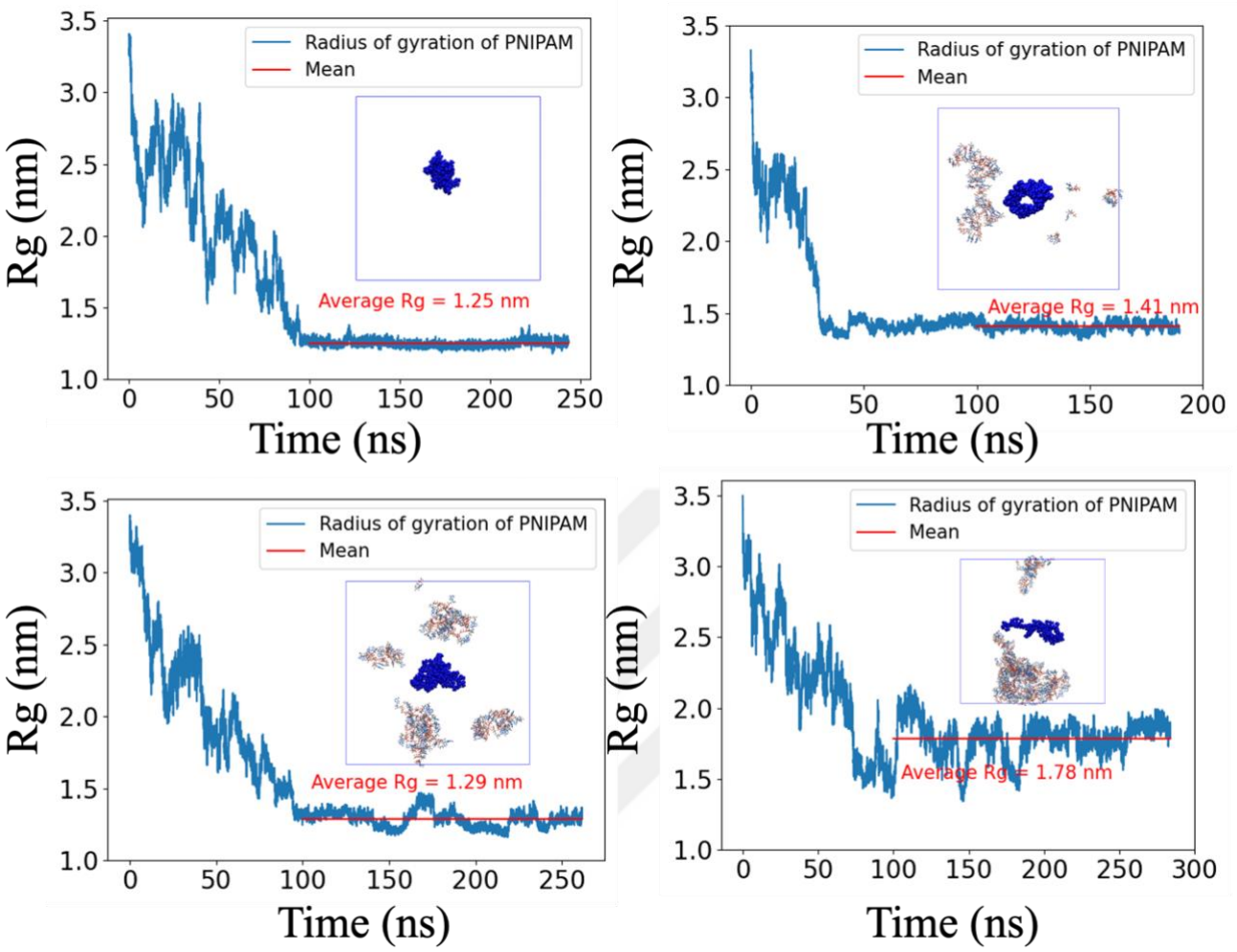


**Figure 3.15:** Radius of gyration values of PNIPAM as a function of time (ns). The inset figures were taken from the 200 ns.

A total of four different simulations were performed, each involving a PNIPAM chain with varying ATP concentrations. The concentrations of ATP investigated were 0 M, 0.1 M, 0.2 M, and 0.3 M. The charge of ATP is neutralized by the addition of $Na^+$ ions, which is parametrized using the Charmm36 force field. The radius of gyration plots of PNIPAM as a function of time for all simulations are illustrated in Figure 3.15, while Figure 3.16 depicts the variation in the radius of gyration of PNIPAM as a function of ATP concentration. Note that,

all three simulations at ATP concentrations of 0 M, 0.2 M, and 0.3 M converged around 100 ns, while the simulation at 0.1M of ATP converged much faster, at around 30 ns. In fact, at around a similar concentration of ATP, the ATR-FTIR measurements also demonstrated an enhanced salting-out mechanism.

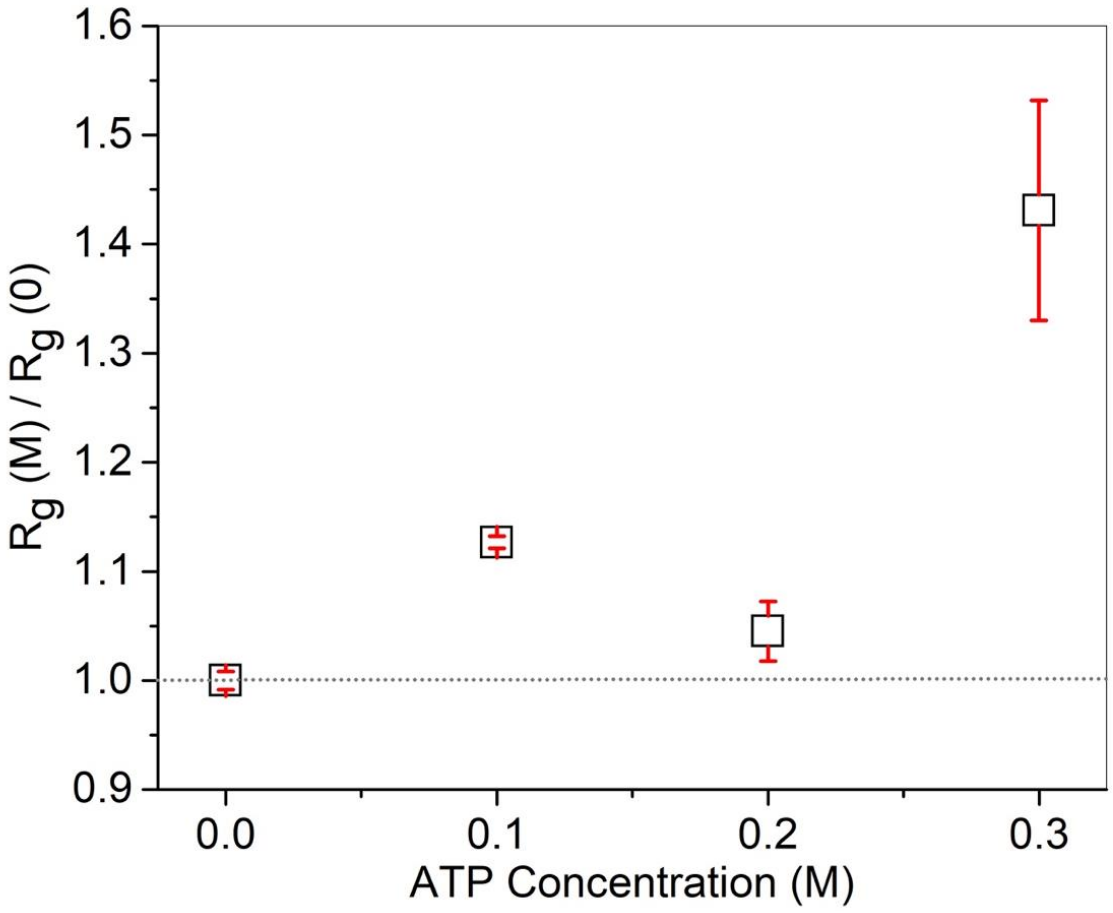


**Figure 3.16:** The ratio of the radius of gyration of PNIPAM in ATP concentration to that in the absence of ATP (0 M), as a function of ATP concentrations: 0 M, 0.1 M, 0.2 M, and 0,3M.

Interestingly, as evident from Figure 3.16, as the ATP concentration further increases, the radius of gyration of the collapsed PNIPAM macromolecule also increases with respect to sole water conditions. At 0.3 M ATP, the variation in the radius of gyration as well as the

average value substantially increases to a value of 1.78 nm. Such simulation results for PNIPAM especially at higher concentrations of ATP can be related to the partial less salting-out seen at higher concentrations of PNIPAM.

### 3.4.1 ATP Clusters

The second major result of the MD simulations is the formation of ATP clustering. In Figure 3.17, snapshots of all four simulations are depicted at 0ns, 125ns, and 250ns, respectively. The start of the simulations for all the ATP concentrations is the same, except for the number of ATP molecules included in the simulation box. The ATP molecule counts in the simulation boxes are as follows: 0 for 0 M ATP, 61 for 0.1 M ATP, 122 for 0.2 M ATP, and 183 for 0.3 M ATP. The snapshots at 125 ns (the half-time of the whole simulation) indicate significant differences in ATP behavior and subtle changes in the shape of the PNIPAM polymer. In the 0.1M ATP simulation, ATP molecules are excluded from the surface of the PNIPAM macromolecule; in other words, they do not make any significant interaction with the polymer. At the 0.2 M ATP concentration, ATP molecules aggregate, forming small clusters that come into contact with the polymer. The aggregation of ATP is much more pronounced in the 0.3 M ATP simulation. Specifically, all the ATP molecules cluster into a few clusters, and they act independently from each other. Moreover, they do not exhibit significant interaction with the PNIPAM polymer. Upon extending the time scale to 250 ns, we observe the formation of ATP clusters even at 0.1 M ATP, further consolidation of ATP clusters at 0.2 M ATP, and the development of large aggregates at 0.3 M ATP concentration. Note that, previous experiments didn't show any hints on the ATP clustering in the aqueous solutions. Yet, the ATP cluster formation that has a non-interacting nature with the

macromolecule in an aqueous solution is quite possible. In fact, the simulation results can provide a potential explanation for the observed decrease in the salting-out behavior of ATP at elevated concentrations, as revealed by the ATR-FTIR experiments. Such significant ATP clustering at higher concentrations could disrupt the larger compartments of the collapse phase of PNIPAM by encroaching upon the spatial arrangement of PNIPAM and compelling it to fragment into smaller aggregates. This can serve as a potential mechanism for why the ratio of PNIPAM aggregation at high concentrations falls below the reference point in Figure 3.10 for the ATR-FTIR measurements.

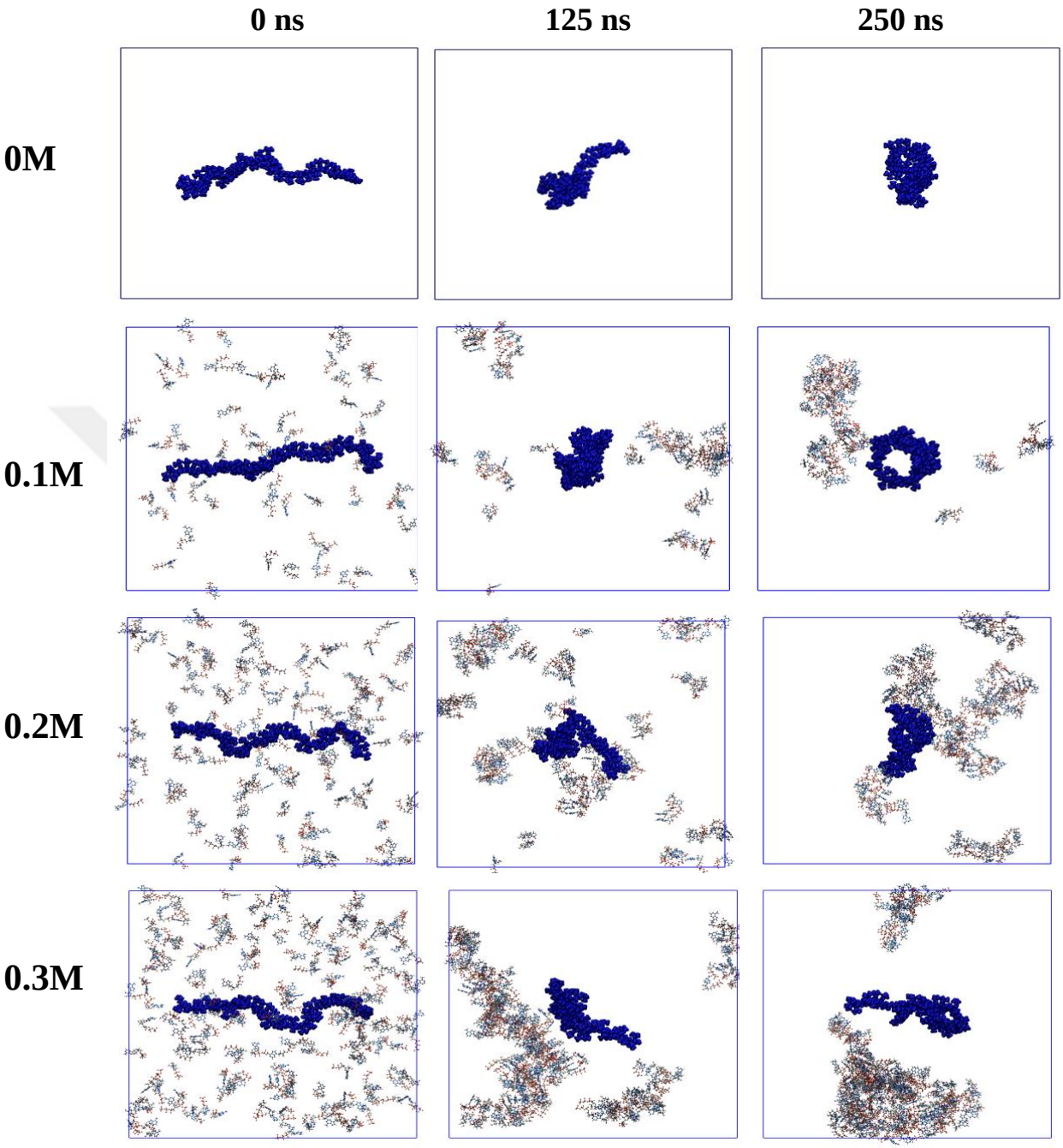


**Figure 3.17:** The screenshots from the four simulations of PNIPAM in ATP solutions: 0.1M, 0.2M, 0.3M ATP, and free-ATP at 0ns, 125ns, and 250ns. The ATP molecule counts in the simulation boxes are as follows: 0 for 0M ATP, 61 for 0.1M ATP, 122 for 0.2M ATP, and 183 for 0.3M ATP.

## 3.5 Multivariate Curve Resolution Raman Spectroscopy

Spectroscopic evidence to demonstrate the clustering of molecules in aqueous solution is quite challenging. In this thesis, by focusing on the hydration shell Raman spectroscopy of ATP molecules, a new method is introduced to report on the clusters of the molecules in aqueous solution. The significance of the hydration shell structure on the stability and functionality of aqueous polymers and biomolecules, including proteins and DNA, has been explored extensively in the literature. [36,164–169] This aspect is noteworthy from both fundamental and practical perspectives. [170,171] The approach integrates high signal-to-noise Raman spectra with multivariate curve resolution, (MCR-Raman), and is applied to dissect two-component solution spectra into a linear combination of pure solvent and solute-correlated (SC) components. The resulting SC spectrum, characterized by a non-negative minimum area, incorporates features originating from both the intramolecular vibrational modes of solute molecules (e.g. C-H vibrational modes) and the perturbations induced by the solute on water OH stretch vibrations. [172–174] The SC spectra offer clear evidence of changes in water hydration structure. This allows for the detection of distinctive characteristics that were not previously visible in the liquid phase of water, such as individual dangling (or "free") OH bonds at the molecular level.

## 3.5.1 Self-Modeling Curve Resolution

The technique employed in this study to extract SC spectra, known as Raman-MCR, utilizes the self-modeling curve resolution (SMCR)[173,175] implemented in IGOR Pro (WaveMetrics). SMCR, as explained earlier, is an analytical approach for decomposing the spectrum of a two-component mixture. Figure 3.18 provides a visual representation of the SMCR decomposition applied to a 0.4 M solution of ATP. Specifically, Figure 3.18a displays the Raman spectra of pure water and a 0.4 M aqueous ATP solution, and the resulting SC spectrum is depicted in Figure 3.18 b.

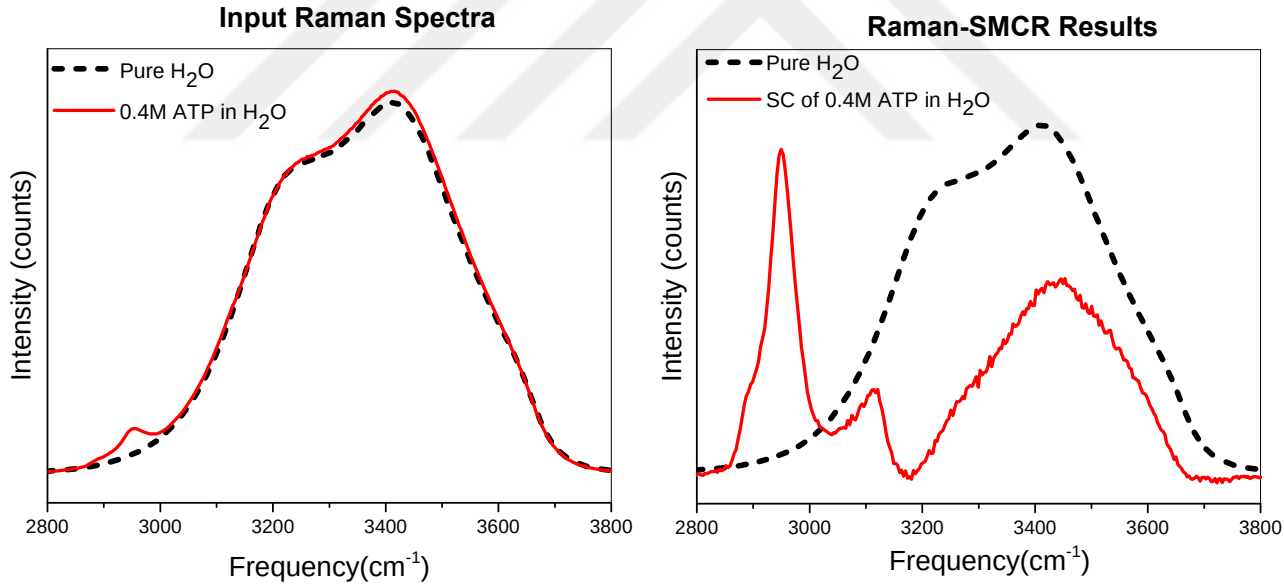


**Figure 3.18: a)** Raman spectra of pure water (dashed black) and 0.4M aqueous ATP solution (red). **b)** SC spectrum of 0.4M ATP (solid red) and Raman spectrum of pure water (black). The features in the SC spectrum arise from the vibrational modes of ATP and water molecules influenced by ATP, displaying differences compared to bulk water.

## 3.5.2 MCR-Raman Measurements: Experimental Investigation of ATP Clustering

To confirm the MD simulation findings of the aggregation behavior of ATP in aqueous solutions experimentally, we conducted Raman-SMCR measurements of aqueous ATP solutions at different concentrations (0.05, 0.1, 0.15,0.2, 0.3, and 0.4 M). The SC spectrum (red curve in Figure 3.18b) originates from intramolecular vibrations of the ATP, including the C-H stretch (at ~2850-3050 $cm^{-1}$), and aromatic C-H (~ 3080 $cm^{-1}$). Additionally, it includes the hydration-shell O-H stretching vibrational features (at ~3170-3800 $cm^{-1}$) resulting from water molecules whose vibrational structure is influenced by the presence of ATP molecules.

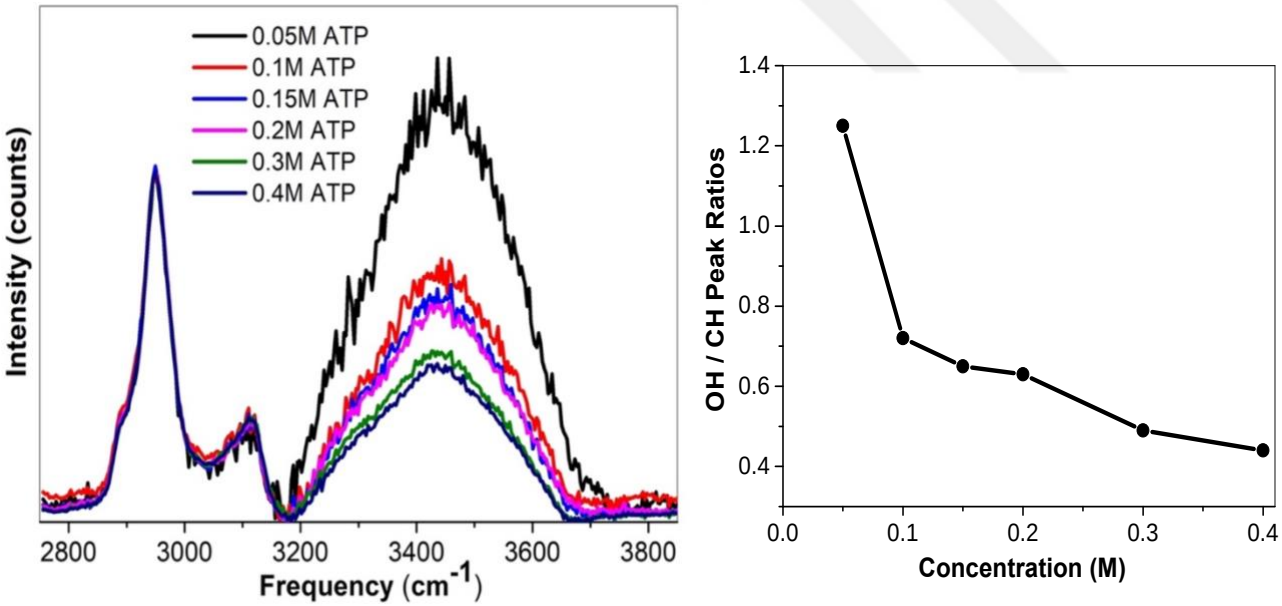


**Figure 3.19: a)** Normalized Raman solute-correlated (SC) spectra of ATP solutions at the concentration range of 0.05 - 0.4M by using Raman multivariate curve resolution analysis. **b)** OH/CH peak ratios as a function of ATP concentration (M).

Figure 3.19a displays the normalized Raman solute-correlated (SC) spectra of ATP solutions within the concentration range of 0.05 to 0.4M, attained through Raman multivariate curve resolution analysis. The spectra vary with the increase of the ATP concentration in the range of ~3170−3690 $cm^{-1}$, corresponding to the OH stretching bands of hydration water. The spectral feature is centered around 3430 $cm^{-1}$, and the intensity of the water band decreases as the concentration of ATP increases. In contrast, the spectra display nearly identical spectral features in the C-H stretching region (~2870-3130 $cm^{-1}$), indicating no shift in the CH vibration of the ATP molecule as its concentration alters. When normalized to the intensity of the C-H stretching band (at 2950 $cm^{-1}$)The resulting SC spectra are clearly distinguished based on the ATP concentration. The intensity of hydrating water bands shows a decreasing trend as the ATP concertation increases. By taking the ratio of the Raman peak intensities of the OH vibration peaks (~3430 $cm^{-1}$) and the CH stretch vibration (~2950 $cm^{-1}$) in the SC spectra, The decrease in the amount of hydration water molecules as a function of ATP is demonstrated in Figure 3.19b. Such a behavior spectral change occurs in the presence of some cluster (aggregation) format, between the molecules. As schematically illustrated in Figure 3.20, a smaller number of water molecules are required to hydrate when molecules cluster in an aqueous solution. In other words, clustering can serve as a dehydration of ATP molecules from their hydration shells. Finally, such clustering should also cause some potential alterations in the SC spectral features.

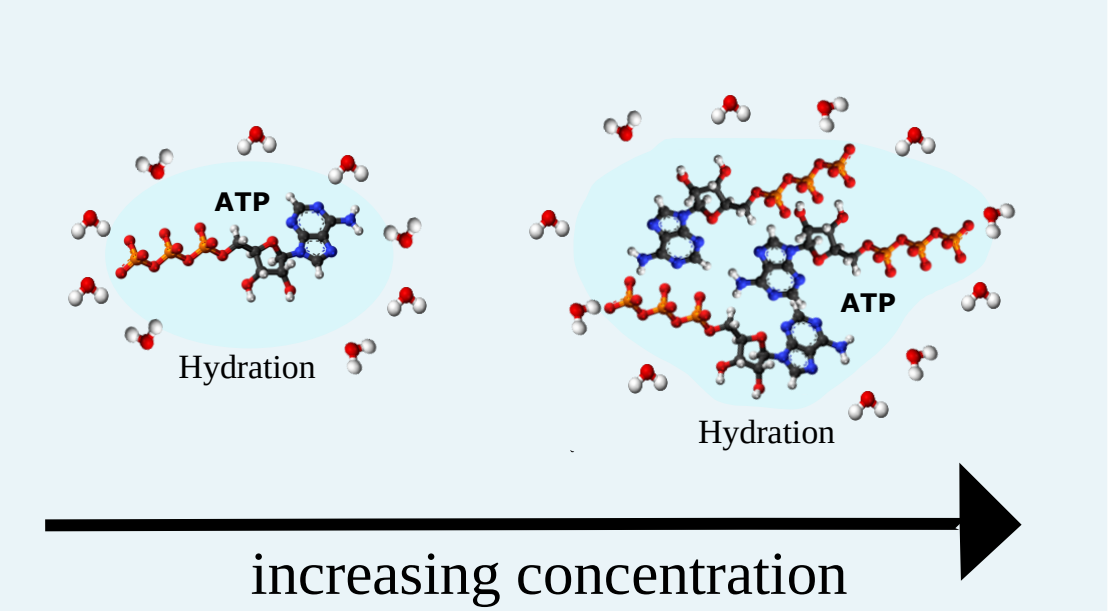


**Figure 3.20:** Schematic illustration of the hydration structure of ATP Molecules: Reduction in Water Quantity per ATP Molecule with Increasing ATP Concentration.

In Figure 3.21, the normalized intensities of the SC hydration spectrum of the O-H vibrational band region are shown. The spectral shape of the O-H region is quite similar as a function of ATP concentration. As the ATP concentration increases the spectral region corresponding to the least coordinated water molecules in the hydration shell gradually diminishes. These water molecules tend to hydrate the more hydrophobic regions of the molecule. As a consequence, the decrease in the hydration of these types of water molecules indicates another type of interaction occurs between these groups on the ATP molecule. Thus, this is the second experimental evidence that ATP molecules form clusters as the concentration increases. The results align with the MD simulation findings, indicating the formation of clusters by ATP molecules.

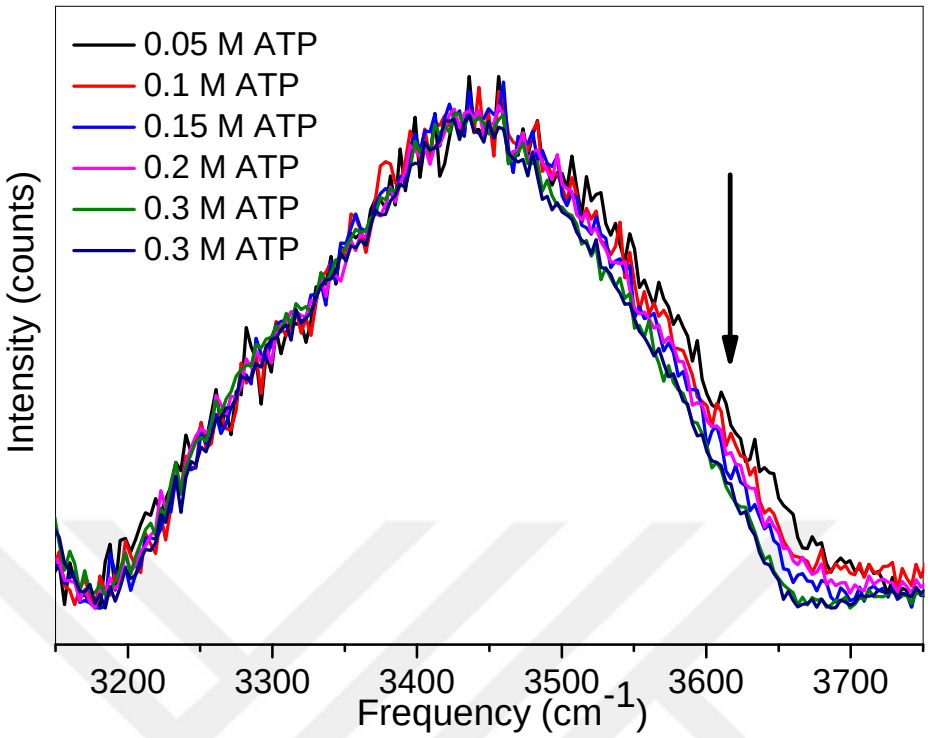


**Figure 3.21:** Raman solute-correlated (SC) spectra of ATP solutions at the concentration range of 0.05-0.4M after performing counterion subtraction by using Raman multivariate curve resolution analysis. The arrow shows the decreasing less-tetrahedrally coordinated water molecules in the hydration shells with increasing ATP concentration.

Overall, all experimental findings consistently point to a unified mechanism. Specifically, phase temperature measurements indicate the salting-out effect of ATP, TP, and AMP on neutral macromolecules with a random coil-like structure, such as PNIPAM. This observation is corroborated by ATR-FTIR measurements at low concentrations of ATP and TP, which are physiologically relevant. Interestingly, at higher concentrations of ATP and its derivatives, the salting-out effect diminishes without a clear underlying cause. Notably, these measurements also demonstrate the exclusion of ATP molecules from the collapsed macromolecule. Furthermore, chemical shift differences in proton signals in NMR measurements suggest the absence of direct binding interactions between ATP / derivatives and any chemical sites on the model macromolecules. The cumulative results from these

experiments suggest that ATP does not function as a hydrotrope; instead, it acts as a stabilizer for neutral amide-based macromolecules with random coil-like structures. The MD simulations at varying ATP concentrations revealed convergence around 30 ns for 0.1 M ATP and approximately 100 ns for 0 M, 0.2 M, and 0.3 M ATP. Concurrent ATR-FTIR measurements demonstrated an augmented salting-out mechanism at a similar ATP concentration, while increasing ATP concentrations correlated with an elevated radius of gyration in the collapsed PNIPAM macromolecule, suggesting a connection to the observed partial salting-out effect at higher PNIPAM concentrations. The MD simulations also revealed a notable result: the formation of ATP clustering. Snapshots at different time points showed increasing aggregation with higher ATP concentrations, leading to significant clusters that acted independently of the PNIPAM polymer. This ATP clustering, not observed in previous experiments in aqueous solutions, provides a potential explanation for the observed decrease in ATP's salting-out behavior at elevated concentrations, as it may disrupt the larger compartments of PNIPAM collapse, leading to smaller aggregates. Finally, to experimentally confirm the aggregation behavior of ATP in aqueous solutions as observed in MD simulations, Raman-SMCR measurements were conducted at various ATP concentrations (0.05 M to 0.4 M). The Raman solute-correlated (SC) spectra revealed changes in the OH stretching bands of hydration water, centered around 3430 $cm^{-1}$, with decreasing intensity as ATP concentration increased. The decrease in hydration water molecules, demonstrated by the ratio of OH vibration peaks to CH stretch vibration, suggests ATP clustering, supported by the consistent spectral changes. This experimental evidence aligns with MD simulation findings, providing further validation for the formation of ATP clusters with increasing concentration.

# Chapter 4 – Conclusion

ATP has been found to act as a biological hydrotrope.[122] A subsequent study [144] highlighted ATP's stabilizing effect on natively folded proteins and salting-in ability on intrinsically disordered proteins. However, the study clarified that neither the salting-out nor salting-in behavior stems from ATP's hydrotropic behavior. Instead, the salting-out effect is attributed to the typical Hofmeister effect, while the salting-in behavior is linked to the specific interaction of adenosine with proteins. In order to shed light on the studied salting-in and salting-out behavior of ATP, we utilized model macromolecules, PNIPAM, and PDEA, that have characteristics of both natively folded proteins and intrinsically folded proteins. These macromolecules contain an amide group along their side chain, and particularly PNIPAM macromolecule contains a valine-like structure with its isopropyl group in its structure. In terms of their chemical structure, they resemble natively folded proteins and are commonly used as a macromolecule model for proteins. However, these macromolecules don't have a defined 3D structure and they have random coil structures like intrinsically disordered proteins do. Hence, PNIPAM and PDEA macromolecules are suitable for the investigation of the salting-in and salting-out behavior of ATP. With this aim, we performed a multi-experimental study and molecular dynamic simulations to elucidate ATP - Biomacromolecule interactions utilizing PNIPAM and PDEA macromolecules. LCST measurements only indicated the salting-out behavior of ATP, TP, and AMP on macromolecules, whereas adenine and adenosine groups didn't significantly influence the phase transition of the macromolecules. ATR-FTIR measurements supported the salting-out behavior of ATP, TP, and AMP molecules, and revealed a surprising decreasing trend in the salting-out behavior of ATP, and TP at high concentrations. AMP, on the other hand, showed a normal salting-out behavior

with a monotonic increase in its salting-out influence. ATR-FTIR measurements also revealed that ATP molecules tend to be excluded from the collapsed form of macromolecules. Additionally, the NMR measurements didn't reveal any site-specific saturable binding between ATP and macromolecules. The snapshots from MD simulations confirmed that there is no significant contact between PNIPAM and ATP molecules. The radius of gyration converged much faster at 0.1 M of ATP in contrast to high concentrations. This kinetic difference is not the scope of this thesis but can potentially be studied in the future. Besides, the 0 - 0.1 M ATP range in the simulations can also be investigated in the later works. The simulations also revealed the ATP clustering, specifically at high concentrations. To confirm the MD simulation results of ATP clustering with experimental data, we conducted MCR-Raman spectroscopy. The solute correlated spectra revealed a decreasing trend in hydration water bands of ATP, which indicates a dehydration occurring between ATP molecules. In other words, there is less water per ATP molecule. This result confirms the ATP clustering and supports the MD simulation results. The formation of ATP clusters at high concentrations might create an additional effect, forcing PNIPAM macromolecules to form smaller aggregates. Our data supports such an explanation for the diminishing salting-out effect of ATP and TP and the increasing errors in the radius of gyration results of PNIPAM at high concentrations. In conclusion, there was no experimental evidence of the salting-in behavior of ATP on macromolecules and site-specific interaction between ATP / derivatives, and the macromolecules. All of these findings concluded that ATP acts as a stabilizer on neutral macromolecules, contradicting its proposed hydrotropic behavior.

# Chapter 5 – References


(1) Perez-gago, M. B.; Krochta, J. M. Denaturation Time and Temperature Effects on Solubility, Tensile Properties, and Oxygen Permeability of Whey Protein Edible Films. J Food Sci 2001, 66 (5), 705–710.

(2) Baldwin, R. L. Temperature Dependence of the Hydrophobic Interaction in Protein Folding. Proceedings of the National Academy of Sciences 1986, 83 (21), 8069–8072.

(3) Zhang, Y.; Furyk, S.; Bergbreiter, D. E.; Cremer, P. S. Specific Ion Effects on the Water Solubility of Macromolecules: PNIPAM and the Hofmeister Series. J Am Chem Soc 2005, 127 (41), 14505–14510.

(4) Lakemond, C. M. M.; de Jongh, H. H. J.; Hessing, M.; Gruppen, H.; Voragen, A. G. J. Soy Glycinin: Influence of PH and Ionic Strength on Solubility and Molecular Structure at Ambient Temperatures. J Agric Food Chem 2000, 48 (6), 1985–1990.

(5) Lo Nostro, P.; Ninham, B. W. Hofmeister Phenomena: An Update on Ion Specificity in Biology. Chem Rev 2012, 112 (4), 2286–2322.

(6) Riès-kautt, M.; Ducruix, A. Inferences Drawn from Physicochemical Studies of Crystallogenesis and Precrystalline State. In Macromolecular Crystallography Part A; Methods in Enzymology; Academic Press, 1997; Vol. 276, pp 23–59.

(7) Baldwin, R. L. How Hofmeister Ion Interactions Affect Protein Stability. Biophys J 1996, 71 (4), 2056–2063.

(8) Zhang, Y.; Cremer, P. Interactions between Macromolecules and Ions: The Hofmeister Series. Curr Opin Chem Biol 2006, 10 (6), 658–663.

(9) Bruce, E. E.; Okur, H. I.; Stegmaier, S.; Drexler, C. I.; Rogers, B. A.; van der Vegt, N. F. A.; Roke, S.; Cremer, P. S. Molecular Mechanism for the Interactions of Hofmeister Cations with Macromolecules in Aqueous Solution. J Am Chem Soc 2020, 142 (45), 19094–19100.

(10) Nomoto, A.; Nishinami, S.; Shiraki, K. Solubility Parameters of Amino Acids on Liquid–Liquid Phase Separation and Aggregation of Proteins. Front Cell Dev Biol 2021, 9.

(11) Yang, Y.; Niroula, A.; Shen, B.; Vihinen, M. PON-Sol: Prediction of Effects of Amino Acid Substitutions on Protein Solubility. Bioinformatics 2016, 32 (13), 2032–2034.

(12) Hou, Q.; Bourgeas, R.; Pucci, F.; Rooman, M. Computational Analysis of the Amino Acid Interactions That Promote or Decrease Protein Solubility. Sci Rep 2018, 8 (1), 14661.

(13) Wang, W. Protein Aggregation and Its Inhibition in Biopharmaceutics. Int J Pharm 2005, 289 (1–2), 1–30.

(14) Arunan, E.; Desiraju, G. R.; Klein, R. A.; Sadlej, J.; Scheiner, S.; Alkorta, I.; Clary, D. C.; Crabtree, R. H.; Dannenberg, J. J.; Hobza, P.; Kjaergaard, H. G.; Legon, A. C.; Mennucci, B.; Nesbitt, D. J. Defining the Hydrogen Bond: An Account (IUPAC Technical Report). Pure and Applied Chemistry 2011, 83 (8), 1619–1636.

(15) Chandler, D. Interfaces and the Driving Force of Hydrophobic Assembly. Nature 2005, 437 (7059), 640–647.

(16) Arnaut, L. Enzymatic Catalysis. In Chemical Kinetics; Elsevier, 2021; pp 409–439.

(17) Schlessinger, J. Cell Signaling by Receptor Tyrosine Kinases. Cell 2000, 103 (2), 211–225.

(18) Litwack, G. Membrane Transport. In Human Biochemistry; Elsevier, 2022; pp 607–645.

(19) Walter, P.; Ron, D. The Unfolded Protein Response: From Stress Pathway to Homeostatic Regulation. Science (1979) 2011, 334 (6059), 1081–1086.

(20) Rothschild, L. J.; Mancinelli, R. L. Life in Extreme Environments. Nature 2001, 409 (6823), 1092–1101.

(21) Levy, Y.; Onuchic, J. N. Water Mediation in Protein Folding and Molecular Recognition. Annu Rev Biophys Biomol Struct 2006, 35 (1), 389–415.

(22) Ball, P. Water as an Active Constituent in Cell Biology. Chem Rev 2008, 108 (1), 74–108.

(23) Kaieda, S.; Halle, B. Internal Water and Microsecond Dynamics in Myoglobin. J Phys Chem B 2013, 117 (47), 14676–14687.

(24) Kuntz, I. D.; Kauzmann, W. Hydration of Proteins and Polypeptides; 1974; pp 239–345.

(25) Laage, D.; Elsaesser, T.; Hynes, J. T. Water Dynamics in the Hydration Shells of Biomolecules. Chem Rev 2017, 117 (16), 10694–10725.

(26) Otting, G.; Liepinsh, E.; Wüthrich, K. Protein Hydration in Aqueous Solution. Science (1979) 1991, 254 (5034), 974–980.

(27) Wiener, M. C.; White, S. H. Structure of a Fluid Dioleoylphosphatidylcholine Bilayer Determined by Joint Refinement of X-Ray and Neutron Diffraction Data. III. Complete Structure. Biophys J 1992, 61 (2), 434–447.

(28) Vlieghe, D.; Turkenburg, J. P.; Van Meervelt, L. B-DNA at Atomic Resolution Reveals Extended Hydration Patterns. Acta Crystallogr D Biol Crystallogr 1999, 55 (9), 1495–1502.

(29) Drew, H. R.; Dickerson, R. E. Structure of a B-DNA Dodecamer. J Mol Biol 1981, 151 (3), 535–556.

(30) Schneider, B.; Patel, K.; Berman, H. M. Hydration of the Phosphate Group in Double-Helical DNA. Biophys J 1998, 75 (5), 2422–2434.

(31) Kumar Pal, S.; H. Zewail, A. Dynamics of Water in Biological Recognition. Chem Rev 2004, 104 (4), 2099–2124.

(32) E. Furse, K.; A. Corcelli, S. The Dynamics of Water at DNA Interfaces: Computational Studies of Hoechst 33258 Bound to DNA. J Am Chem Soc 2008, 130 (39), 13103–13109.

(33) Yang, M.; Szyc, Ł.; Elsaesser, T. Decelerated Water Dynamics and Vibrational Couplings of Hydrated DNA Mapped by Two-Dimensional Infrared Spectroscopy. J Phys Chem B 2011, 115 (44), 13093–13100.

(34) Halle, B.; Nilsson, L. Does the Dynamic Stokes Shift Report on Slow Protein Hydration Dynamics? J Phys Chem B 2009, 113 (24), 8210–8213.

(35) Zhong, D.; Pal, S. K.; Zewail, A. H. Biological Water: A Critique. Chem Phys Lett 2011, 503 (1–3), 1–11.

(36) Levy, Y.; Onuchic, J. N. Water Mediation in Protein Folding and Molecular Recognition. Annu Rev Biophys Biomol Struct 2006, 35 (1), 389–415.

(37) Di Russo, N. V.; Estrin, D. A.; Martí, M. A.; Roitberg, A. E. PH-Dependent Conformational Changes in Proteins and Their Effect on Experimental PKas: The Case of Nitrophorin 4. PLoS Comput Biol 2012, 8 (11), e1002761.

(38) Shang, L.; Wang, Y.; Jiang, J.; Dong, S. PH-Dependent Protein Conformational Changes in Albumin:Gold Nanoparticle Bioconjugates: A Spectroscopic Study. Langmuir 2007, 23 (5), 2714–2721.

(39) Ota, C.; Fukuda, Y.; Tanaka, S.; Takano, K. Spectroscopic Evidence of the Salt-Induced Conformational Change around the Localized Electric Charges on the Protein Surface of Fibronectin Type III. Langmuir 2020, 36 (47), 14243–14254.

(40) Formaneck, M. S.; Ma, L.; Cui, Q. Effects of Temperature and Salt Concentration on the Structural Stability of Human Lymphotactin: Insights from Molecular Simulations. J Am Chem Soc 2006, 128 (29), 9506–9517.

(41) Kukic, P.; O'Meara, F.; Hewage, C.; Erik Nielsen, J. Coupled Effect of Salt and PH on Proteins Probed with NMR Spectroscopy. Chem Phys Lett 2013, 579, 114–121.

(42) Berezovskaya, Y.; Porrini, M.; Barran, P. E. The Effect of Salt on the Conformations of Three Model Proteins Is Revealed by Variable Temperature Ion Mobility Mass Spectrometry. Int J Mass Spectrom 2013, 345–347, 8–18.

(43) Reyes-Alcaraz, A.; Martínez-Archundia, M.; Ramon, E.; Garriga, P. Salt Effects on the Conformational Stability of the Visual G-Protein-Coupled Receptor Rhodopsin. Biophys J 2011, 101 (11), 2798–2806.

(44) Okur, H. I.; Hladílková, J.; Rembert, K. B.; Cho, Y.; Heyda, J.; Dzubiella, J.; Cremer, P. S.; Jungwirth, P. Beyond the Hofmeister Series: Ion-Specific Effects on Proteins and Their Biological Functions. J Phys Chem B 2017, 121 (9), 1997–2014.

(45) Hofmeister, F. Zur Lehre von Der Wirkung Der Salze. Archiv für Experimentelle Pathologie und Pharmakologie 1888, 24 (4–5), 247–260.

(46) Jungwirth, P.; Cremer, P. S. Beyond Hofmeister. Nat Chem 2014, 6 (4), 261–263.

(47) Xie, W. J.; Gao, Y. Q. A Simple Theory for the Hofmeister Series. J Phys Chem Lett 2013, 4 (24), 4247–4252.

(48) Schwierz, N.; Horinek, D.; Netz, R. R. Anionic and Cationic Hofmeister Effects on Hydrophobic and Hydrophilic Surfaces. Langmuir 2013, 29 (8), 2602–2614.

(49) Pegram, L. M.; Record, M. T. Thermodynamic Origin of Hofmeister Ion Effects. J Phys Chem B 2008, 112 (31), 9428–9436.

(50) Kunz, W.; Lo Nostro, P.; Ninham, B. W. The Present State of Affairs with Hofmeister Effects. Curr Opin Colloid Interface Sci 2004, 9 (1–2), 1–18.

(51) Thomas Record, M.; Zhang, W.; Anderson, C. F. Analysis of Effects of Salts and Uncharged Solutes on Protein and Nucleic Acid Equilibria and Processes: A Practical Guide to Recognizing and Interpreting Polyelectrolyte Effects, Hofmeister Effects, and Osmotic Effects of Salts; 1998; pp 281–353.

(52) Cacace, M. G.; Landau, E. M.; Ramsden, J. J. The Hofmeister Series: Salt and Solvent Effects on Interfacial Phenomena. Q Rev Biophys 1997, 30 (3), S0033583597003363.

(53) Fruton, J. S. Contrasts in Scientific Style. Emil Fischer and Franz Hofmeister: Their Research Groups and Their Theory of Protein Structure. Proc Am Philos Soc 1985, 129 (4), 313–370.

(54) Collins, K. D.; Washabaugh, M. W. The Hofmeister Effect and the Behaviour of Water at Interfaces. Q Rev Biophys 1985, 18 (4), 323–422.

(55) Leo Abernethy, J. Franz Hofmeister - The Impact of His Life and Research on Chemistry. J Chem Educ 1967, 44 (3).

(56) Schwierz, N.; Horinek, D.; Sivan, U.; Netz, R. R. Reversed Hofmeister Series—The Rule Rather than the Exception. Curr Opin Colloid Interface Sci 2016, 23, 10–18.

(57) Lo Nostro, P.; Ninham, B. W. Editorial: Electrolytes and Specific Ion Effects. New and Old Horizons. Curr Opin Colloid Interface Sci 2016, 23, A1–A5.

(58) Zhang, Y.; Cremer, P. Interactions between Macromolecules and Ions: The Hofmeister Series. Curr Opin Chem Biol 2006, 10 (6), 658–663.

(59) Arrhenius Svante. Recherches Sur La Conductibilité Galvanique Des Électrolytes., University of Uppsala, Norstedt & Söner, 1884.

(60) Hofmeister, F. Zur Lehre von Der Wirkung Der Salze. Archiv für Experimentelle Pathologie und Pharmakologie 1888, 25, 1–30.

(61) Kropman, M. F.; Bakker, H. J. Dynamics of Water Molecules in Aqueous Solvation Shells. Science (1979) 2001, 291 (5511), 2118–2120.

(62) Kropman, M. F.; Bakker, H. J. Vibrational Relaxation of Liquid Water in Ionic Solvation Shells. Chem Phys Lett 2003, 370 (5–6), 741–746.

(63) Omta, A. W.; Kropman, M. F.; Woutersen, S.; Bakker, H. J. Influence of Ions on the Hydrogen-Bond Structure in Liquid Water. J Chem Phys 2003, 119 (23), 12457–12461.

(64) Kropman, M. F.; Bakker, H. J. Femtosecond Mid-Infrared Spectroscopy of Aqueous Solvation Shells. J Chem Phys 2001, 115 (19), 8942–8948.

(65) F. Kropman, M.; J. Bakker, H. Effect of Ions on the Vibrational Relaxation of Liquid Water. J Am Chem Soc 2004, 126 (29), 9135–9141.

(66) Omta, A. W.; Kropman, M. F.; Woutersen, S.; Bakker, H. J. Negligible Effect of Ions on the Hydrogen-Bond Structure in Liquid Water. Science (1979) 2003, 301 (5631), 347–349.

(67) D. Batchelor, J.; Olteanu, A.; Tripathy, A.; J. Pielak, G. Impact of Protein Denaturants and Stabilizers on Water Structure. J Am Chem Soc 2004, 126 (7), 1958–1961.

(68) E. Gragson, D.; M. McCarty, B.; L. Richmond, G. Ordering of Interfacial Water Molecules at the Charged Air/Water Interface Observed by Vibrational Sum Frequency Generation. J Am Chem Soc 1997, 119 (26), 6144–6152.

(69) B. Miranda, P.; R. Shen, Y. Liquid Interfaces: A Study by Sum-Frequency Vibrational Spectroscopy. J Phys Chem B 1999, 103 (17), 3292–3307.

(70) Shen, Y. R. Surface Properties Probed by Second-Harmonic and Sum-Frequency Generation. Nature 1989, 337 (6207), 519–525.

(71) Zhang, Y.; Cremer, P. S. The Inverse and Direct Hofmeister Series for Lysozyme. Proceedings of the National Academy of Sciences 2009, 106 (36), 15249–15253.

(72) Robertson, T. B. Contributions to the Theory of the Mode of Action of Inorganic Salts upon Proteins in Solution. Journal of Biological Chemistry 1911, 9 (3), 303–326.

(73) Ries-Kautt, M. M.; Ducruix, A. F. Relative Effectiveness of Various Ions on the Solubility and Crystal Growth of Lysozyme. J Biol Chem 1989, 264 (2), 745–748.

(74) Hamabata, A.; H. Von Hippel, P. Model Studies on the Effects of Neutral Salts on the Conformational Stability of Biological Macromolecules. II. Effects of Vicinal Hydrophobic Groups on the Specificity of Binding of Ions to Amide Groups. Biochemistry 2002, 12 (7), 1264–1271.

(75) K. Nandi, P.; R. Robinson, D. Effects of Salts on the Free Energy of the Peptide Group. J Am Chem Soc 2002, 94 (4), 1299–1308.

(76) R. Robinson, D.; P. Jencks, W. The Effect of Concentrated Salt Solutions on the Activity Coefficient of Acetyltetraglycine Ethyl Ester. J Am Chem Soc 2002, 87 (11), 2470–2479.

(77) Chi, E. Y.; Krishnan, S.; Randolph, T. W.; Carpenter, J. F. Physical Stability of Proteins in Aqueous Solution: Mechanism and Driving Forces in Nonnative Protein Aggregation. Pharm Res 2003, 20 (9), 1325–1336.

(78) Burg, M. B.; Ferraris, J. D. Intracellular Organic Osmolytes: Function and Regulation. Journal of Biological Chemistry 2008, 283 (12), 7309–7313.

(79) Mahler, H.-C.; Friess, W.; Grauschopf, U.; Kiese, S. Protein Aggregation: Pathways, Induction Factors and Analysis. J Pharm Sci 2009, 98 (9), 2909–2934.

(80) Cromwell, M. E. M.; Hilario, E.; Jacobson, F. Protein Aggregation and Bioprocessing. AAPS J 2006, 8 (3), E572–E579.

(81) Rosenberg, A. S. Effects of Protein Aggregates: An Immunologic Perspective. AAPS J 2006, 8 (3), E501–E507.

(82) Macielag, M. J. Chemical Properties of Antimicrobials and Their Uniqueness. In Antibiotic Discovery and Development; Springer US: Boston, MA, 2012; pp 793–820.

(83) Visnes, T.; Cázares-Körner, A.; Hao, W.; Wallner, O.; Masuyer, G.; Loseva, O.; Mortusewicz, O.; Wiita, E.; Sarno, A.; Manoilov, A.; Astorga-Wells, J.; Jemth, A.-S.; Pan, L.; Sanjiv, K.; Karsten, S.; Gokturk, C.; Grube, M.; Homan, E. J.; Hanna, B. M. F.; Paulin, C. B. J.; Pham, T.; Rasti, A.; Berglund, U. W.; von Nicolai, C.; Benitez-Buelga, C.; Koolmeister, T.; Ivanic, D.; Iliev, P.; Scobie, M.; Krokan, H. E.;

Baranczewski, P.; Artursson, P.; Altun, M.; Jensen, A. J.; Kalderén, C.; Ba, X.; Zubarev, R. A.; Stenmark, P.; Boldogh, I.; Helleday, T. Small-Molecule Inhibitor of OGG1 Suppresses Proinflammatory Gene Expression and Inflammation. Science (1979) 2018, 362 (6416), 834–839.

(84) Wang, B.; Barahona, M.; Buck, M. Amplification of Small Molecule-Inducible Gene Expression via Tuning of Intracellular Receptor Densities. Nucleic Acids Res 2015, 43 (3), 1955–1964.

(85) Banerjee, D.; Zhao, L.; Wu, L.; Palanichamy, A.; Ergun, A.; Peng, L.; Quigley, C.; Hamann, S.; Dunstan, R.; Cullen, P.; Allaire, N.; Guertin, K.; Wang, T.; Chao, J.; Loh, C.; Fontenot, J. D. Small Molecule Mediated Inhibition of <scp>ROR</Scp> γ -dependent Gene Expression and Autoimmune Disease Pathology in Vivo. Immunology 2016, 147 (4), 399–413.

(86) Song, J.; Malampati, S.; Zeng, Y.; Durairajan, S. S. K.; Yang, C.; Tong, B. C.; Iyaswamy, A.; Shang, W.; Sreenivasmurthy, S. G.; Zhu, Z.; Cheung, K.; Lu, J.; Tang, C.; Xu, N.; Li, M. A Small Molecule Transcription Factor EB Activator Ameliorates Beta-amyloid Precursor Protein and Tau Pathology in Alzheimer's Disease Models. Aging Cell 2020, 19 (2).

(87) Hurtado, C.; Safarova, A.; Smith, M.; Chung, R.; Bruyneel, A. A. N.; Gomez-Galeno, J.; Oswald, F.; Larson, C. J.; Cashman, J. R.; Ruiz-Lozano, P.; Janiak, P.; Suzuki, T.; Mercola, M. Disruption of NOTCH Signaling by a Small Molecule Inhibitor of the Transcription Factor RBPJ. Sci Rep 2019, 9 (1), 10811.

(88) Taylor, A.; Rothstein, D.; Rudd, C. E. Small-Molecule Inhibition of PD-1 Transcription Is an Effective Alternative to Antibody Blockade in Cancer Therapy. Cancer Res 2018, 78 (3), 706–717.

(89) Zhang, P.; Park, H.-J.; Zhang, J.; Junn, E.; Andrews, R. J.; Velagapudi, S. P.; Abegg, D.; Vishnu, K.; Costales, M. G.; Childs-Disney, J. L.; Adibekian, A.; Moss, W. N.; Mouradian, M. M.; Disney, M. D. Translation of the Intrinsically Disordered Protein α-Synuclein Is Inhibited by a Small Molecule Targeting Its Structured MRNA. Proceedings of the National Academy of Sciences 2020, 117 (3), 1457–1467.

(90) Hagler, L. D.; Bonson, S. E.; Kocheril, P. A.; Zimmerman, S. C. Assessing the Feasibility and Stability of Uracil Base Flipping in RNA–Small Molecule Complexes Using Molecular Dynamics Simulations. Can J Chem 2020, 98 (6), 261–269.

(91) Ramadass, V.; Vaiyapuri, T.; Tergaonkar, V. Small Molecule NF-KB Pathway Inhibitors in Clinic. Int J Mol Sci 2020, 21 (14), 5164.

(92) Chen, H.; Bian, A.; Yang, L.; Yin, X.; Wang, J.; Ti, C.; Miao, Y.; Peng, S.; Xu, S.; Liu, M.; Qiu, W.-W.; Yi, Z. Targeting STAT3 by a Small Molecule Suppresses Pancreatic Cancer Progression. Oncogene 2021, 40 (8), 1440–1457.

(93) Yancey, P. H.; Clark, M. E.; Hand, S. C.; Bowlus, R. D.; Somero, G. N. Living with Water Stress: Evolution of Osmolyte Systems. Science (1979) 1982, 217 (4566), 1214–1222.

(94) Rani, A.; Venkatesu, P. Changing Relations between Proteins and Osmolytes: A Choice of Nature. Physical Chemistry Chemical Physics 2018, 20 (31), 20315–20333.

(95) Carpenter, J. F.; Kendrick, B. S.; Chang, B. S.; Manning, M. C.; Randolph, T. W. [16] Inhibition of Stress-Induced Aggregation of Protein Therapeutics; 1999; pp 236–255.

(96) Greene, R. F.; Pace, C. N. Urea and Guanidine Hydrochloride Denaturation of Ribonuclease, Lysozyme, α-Chymotrypsin, and b-Lactoglobulin. Journal of Biological Chemistry 1974, 249 (17), 5388–5393.

(97) Makhatadze, G. I.; Privalov, P. L. Protein Interactions with Urea and Guanidinium Chloride. J Mol Biol 1992, 226 (2), 491–505.

(98) Pace, C. N. [14]Determination and Analysis of Urea and Guanidine Hydrochloride Denaturation Curves; 1986; pp 266–280.

(99) Robinson, D. R.; Jencks, W. P. The Effect of Compounds of the Urea-Guanidinium Class on the Activity Coefficient of Acetyltetraglycine Ethyl Ester and Related Compounds 1. J Am Chem Soc 1965, 87 (11), 2462–2470.

(100) Mason, P. E.; Brady, J. W.; Neilson, G. W.; Dempsey, C. E. The Interaction of Guanidinium Ions with a Model Peptide. Biophys J 2007, 93 (1), L04–L06.

(101) P. O'Brien, E.; I. Dima, R.; Brooks, B.; Thirumalai, D. Interactions between Hydrophobic and Ionic Solutes in Aqueous Guanidinium Chloride and Urea Solutions: Lessons for Protein Denaturation Mechanism. J Am Chem Soc 2007, 129 (23), 7346–7353.

(102) Das, A.; Mukhopadhyay, C. Urea-Mediated Protein Denaturation: A Consensus View. J Phys Chem B 2009, 113 (38), 12816–12824.

(103) Hanna, C. C.; Kriegesmann, J.; Dowman, L. J.; Becker, C. F. W.; Payne, R. J. Chemical Synthesis and Semisynthesis of Lipidated Proteins. Angewandte Chemie International Edition 2022, 61 (15).

(104) Heyda, J.; Okur, H. I.; Hladílková, J.; Rembert, K. B.; Hunn, W.; Yang, T.; Dzubiella, J.; Jungwirth, P.; Cremer, P. S. Guanidinium Can Both Cause and Prevent the

Hydrophobic Collapse of Biomacromolecules. J Am Chem Soc 2017, 139 (2), 863–870.

(105) E. Mason, P.; Wernersson, E.; Jungwirth, P. Accurate Description of Aqueous Carbonate Ions: An Effective Polarization Model Verified by Neutron Scattering. J Phys Chem B 2012, 116 (28), 8145–8153.

(106) Heyda, J.; Kožíšek, M.; Bednárova, L.; Thompson, G.; Konvalinka, J.; Vondrášek, J.; Jungwirth, P. Urea and Guanidinium Induced Denaturation of a Trp-Cage Miniprotein. J Phys Chem B 2011, 115 (28), 8910–8924.

(107) Street, T. O.; Bolen, D. W.; Rose, G. D. A Molecular Mechanism for Osmolyte-Induced Protein Stability. Proceedings of the National Academy of Sciences 2006, 103 (38), 13997–14002.

(108) Trevino, S. R.; Scholtz, J. M.; Pace, C. N. Measuring and Increasing Protein Solubility. J Pharm Sci 2008, 97 (10), 4155–4166.

(109) Jaspe, J.; Hagen, S. J. Do Protein Molecules Unfold in a Simple Shear Flow? Biophys J 2006, 91 (9), 3415–3424.

(110) Brown, J. Application of Molecular Genetics to the Diagnosis of Inherited Diseases. Biochem Educ 1992, 20 (2), 121.

(111) Didierjean, C.; Tête-Favier, F. Introduction to Protein Science. Architecture, Function and Genomics. Third Edition. By Arthur M. Lesk. Oxford University Press, 2016. Pp. 466. Paperback. Price GBP 39.99. ISBN 9780198716846. Acta Crystallogr D Struct Biol 2016, 72 (12), 1308–1309.

(112) Bauduin, P.; Renoncourt, A.; Kopf, A.; Touraud, D.; Kunz, W. Unified Concept of Solubilization in Water by Hydrotropes and Cosolvents. Langmuir 2005, 21 (15), 6769–6775.

(113) Neuberg, C. Hydrotropic Phenomena. Biochem 1916, 76, 107–176.

(114) Hodgdon, T. K.; Kaler, E. W. Hydrotropic Solutions. Curr Opin Colloid Interface Sci 2007, 12 (3), 121–128.

(115) Shimizu, S.; Nagai Kanasaki, Y. Effect of Solute Aggregation on Solubilization. J Mol Liq 2019, 274, 209–214.

(116) Booth, J. J.; Abbott, S.; Shimizu, S. Mechanism of Hydrophobic Drug Solubilization by Small Molecule Hydrotropes. J Phys Chem B 2012, 116 (51), 14915–14921.

(117) Srinivas, V.; Rodley, G. A.; Ravikumar, K.; Robinson, W. T.; Turnbull, M. M. Molecular Organization in Hydrotrope Assemblies. Langmuir 1997, 13 (12), 3235–3239.

(118) Hopkins Hatzopoulos, M.; Eastoe, J.; Dowding, P. J.; Rogers, S. E.; Heenan, R.; Dyer, R. Are Hydrotropes Distinct from Surfactants? Langmuir 2011, 27 (20), 12346–12353.

(119) Kunz, W.; Holmberg, K.; Zemb, T. Hydrotropes. Curr Opin Colloid Interface Sci 2016, 22, 99–107.

(120) Mehringer, J.; Hofmann, E.; Touraud, D.; Koltzenburg, S.; Kellermeier, M.; Kunz, W. Salting-in and Salting-out Effects of Short Amphiphilic Molecules: A Balance between Specific Ion Effects and Hydrophobicity. Physical Chemistry Chemical Physics 2021, 23 (2), 1381–1391.

(121) Friberg, S. E.; Chiu, M. HYDROTROPES. J Dispers Sci Technol 1988, 9 (5), 443–457.

(122) Patel, A.; Malinovska, L.; Saha, S.; Wang, J.; Alberti, S.; Krishnan, Y.; Hyman, A. A. ATP as a Biological Hydrotrope. Science (1979) 2017, 356 (6339), 753–756.

(123) Khakh, B. S.; Burnstock, G. The Double Life of ATP. Sci Am 2009, 301 (6), 84–92.

(124) Bonora, M.; Patergnani, S.; Rimessi, A.; De Marchi, E.; Suski, J. M.; Bononi, A.; Giorgi, C.; Marchi, S.; Missiroli, S.; Poletti, F.; Wieckowski, M. R.; Pinton, P. ATP Synthesis and Storage. Purinergic Signal 2012, 8 (3), 343–357.

(125) Burnstock, G. Historical Review: ATP as a Neurotransmitter. Trends Pharmacol Sci 2006, 27 (3), 166–176.

(126) Di Virgilio, F.; Sarti, A. C.; Falzoni, S.; De Marchi, E.; Adinolfi, E. Extracellular ATP and P2 Purinergic Signalling in the Tumour Microenvironment. Nat Rev Cancer 2018, 18 (10), 601–618.

(127) Gordon, J. L. Extracellular ATP: Effects, Sources and Fate. Biochemical Journal 1986, 233 (2), 309–319.

(128) Vultaggio-Poma, V.; Sarti, A. C.; Di Virgilio, F. Extracellular ATP: A Feasible Target for Cancer Therapy. Cells 2020, 9 (11), 2496.

(129) Kojima, S.; Ohshima, Y.; Nakatsukasa, H.; Tsukimoto, M. Role of ATP as a Key Signaling Molecule Mediating Radiation-Induced Biological Effects. Dose-Response 2017, 15 (1), 155932581769063.

(130) Dunn, J.; Grider, M. H. Physiology, Adenosine Triphosphate; 2023.

(131) Granot, J.; Rosenheck, K. On the Role of ATP and Divalent Metal Ions in the Storage of Catecholamines. FEBS Lett 1978, 95 (1), 45–48.

(132) FRAUSTO DA SILVA, J. J. R.; WILLIAMS, R. J. P. Possible Mechanism for the Biological Action of Lithium. Nature 1976, 263 (5574), 237–239.

(133) Weber, A.; Winkler, H. Specificity and Mechanism of Nucleotide Uptake by Adrenal Chromaffin Granules. Neuroscience 1981, 6 (11), 2269–2276.

(134) Banani, S. F.; Lee, H. O.; Hyman, A. A.; Rosen, M. K. Biomolecular Condensates: Organizers of Cellular Biochemistry. Nat Rev Mol Cell Biol 2017, 18 (5), 285–298.

(135) Jain, S.; Wheeler, J. R.; Walters, R. W.; Agrawal, A.; Barsic, A.; Parker, R. ATPase-Modulated Stress Granules Contain a Diverse Proteome and Substructure. Cell 2016, 164 (3), 487–498.

(136) Alberti, S.; Dormann, D. Liquid–Liquid Phase Separation in Disease. Annu Rev Genet 2019, 53 (1), 171–194.

(137) Yu, H.; Lu, S.; Gasior, K.; Singh, D.; Vazquez-Sanchez, S.; Tapia, O.; Toprani, D.; Beccari, M. S.; Yates, J. R.; Da Cruz, S.; Newby, J. M.; Lafarga, M.; Gladfelter, A. S.; Villa, E.; Cleveland, D. W. HSP70 Chaperones RNA-Free TDP-43 into Anisotropic Intranuclear Liquid Spherical Shells. Science (1979) 2021, 371 (6529).

(138) Kurisaki, I.; Tanaka, S. ATP Converts Aβ 42 Oligomer into Off-Pathway Species by Making Contact with Its Backbone Atoms Using Hydrophobic Adenosine. J Phys Chem B 2019, 123 (46), 9922–9933.

(139) Kang, J.; Lim, L.; Song, J. ATP Binds and Inhibits the Neurodegeneration-Associated Fibrillization of the FUS RRM Domain. Commun Biol 2019, 2 (1), 223.

(140) Dang, M.; Kang, J.; Lim, L.; Li, Y.; Wang, L.; Song, J. ATP Is a Cryptic Binder of TDP-43 RRM Domains to Enhance Stability and Inhibit ALS/AD-Associated Fibrillation. Biochem Biophys Res Commun 2020, 522 (1), 247–253.

(141) He, Y.; Kang, J.; Song, J. ATP Antagonizes the Crowding-Induced Destabilization of the Human Eye-Lens Protein ΓS-Crystallin. Biochem Biophys Res Commun 2020, 526 (4), 1112–1117.

(142) Hayes, M. H.; Peuchen, E. H.; Dovichi, N. J.; Weeks, D. L. Dual Roles for ATP in the Regulation of Phase Separated Protein Aggregates in Xenopus Oocyte Nucleoli. Elife 2018, 7.

(143) Sridharan, S.; Kurzawa, N.; Werner, T.; Günthner, I.; Helm, D.; Huber, W.; Bantscheff, M.; Savitski, M. M. Proteome-Wide Solubility and Thermal Stability Profiling Reveals Distinct Regulatory Roles for ATP. Nat Commun 2019, 10 (1), 1155.

(144) Mehringer, J.; Do, T.-M.; Touraud, D.; Hohenschutz, M.; Khoshsima, A.; Horinek, D.; Kunz, W. Hofmeister versus Neuberg: Is ATP Really a Biological Hydrotrope? Cell Rep Phys Sci 2021, 2 (2), 100343.

(145) Song, J. Adenosine Triphosphate Energy-independently Controls Protein Homeostasis with Unique Structure and Diverse Mechanisms. Protein Science 2021, 30 (7), 1277–1293.

(146) Dang, M.; Li, Y.; Song, J. Tethering-Induced Destabilization and ATP-Binding for Tandem RRM Domains of ALS-Causing TDP-43 and HnRNPA1. Sci Rep 2021, 11 (1), 1034.

(147) Kang, J.; Lim, L.; Lu, Y.; Song, J. A Unified Mechanism for LLPS of ALS/FTLD-Causing FUS as Well as Its Modulation by ATP and Oligonucleic Acids. PLoS Biol 2019, 17 (6), e3000327.

(148) Kang, J.; Lim, L.; Song, J. ATP Enhances at Low Concentrations but Dissolves at High Concentrations Liquid-Liquid Phase Separation (LLPS) of ALS/FTD-Causing FUS. Biochem Biophys Res Commun 2018, 504 (2), 545–551.

(149) Dang, M.; Song, J. ALS-Causing D169G Mutation Disrupts the ATP-Binding Capacity of TDP-43 RRM1 Domain. Biochem Biophys Res Commun 2020, 524 (2), 459–464.

(150) Nishizawa, M.; Walinda, E.; Morimoto, D.; Kohn, B.; Scheler, U.; Shirakawa, M.; Sugase, K. Effects of Weak Nonspecific Interactions with ATP on Proteins. J Am Chem Soc 2021, 143 (31), 11982–11993.

(151) Bye, J. W.; Curtis, R. A. Controlling Phase Separation of Lysozyme with Polyvalent Anions. J Phys Chem B 2019, 123 (3), 593–605. https://doi.org/10.1021/acs.jpcb.8b10868.

(152) Lenton, S.; Hervø-Hansen, S.; Popov, A. M.; Tully, M. D.; Lund, M.; Skepö, M. Impact of Arginine–Phosphate Interactions on the Reentrant Condensation of Disordered Proteins. Biomacromolecules 2021, 22 (4), 1532–1544.

(153) Heo, C. E.; Han, J. Y.; Lim, S.; Lee, J.; Im, D.; Lee, M. J.; Kim, Y. K.; Kim, H. I. ATP Kinetically Modulates Pathogenic Tau Fibrillations. ACS Chem Neurosci 2020, 11 (19), 3144–3152.

(154) Dec, R.; Puławski, W.; Dzwolak, W. Selective and Stoichiometric Incorporation of ATP by Self-Assembling Amyloid Fibrils. J Mater Chem B 2021, 9 (41), 8626–8630.

(155) Roy, D.; Brooks, W. L. A.; Sumerlin, B. S. New Directions in Thermoresponsive Polymers. Chem Soc Rev 2013, 42 (17), 7214.

(156) Schild, H. G. Poly(N-Isopropylacrylamide): Experiment, Theory and Application. Prog Polym Sci 1992, 17 (2), 163–249.

(157) Tiktopulo, E. I.; Uversky, V. N.; Lushchik, V. B.; Klenin, S. I.; Bychkova, V. E.; Ptitsyn, O. B. "Domain" Coil-Globule Transition in Homopolymers. Macromolecules 1995, 28 (22), 7519–7524.

(158) Deshmukh, S. A.; Sankaranarayanan, S. K. R. S.; Suthar, K.; Mancini, D. C. Role of Solvation Dynamics and Local Ordering of Water in Inducing Conformational Transitions in Poly( N -Isopropylacrylamide) Oligomers through the LCST. J Phys Chem B 2012, 116 (9), 2651–2663.

(159) Aseyev, V. O.; Tenhu, H.; Winnik, F. M. Temperature Dependence of the Colloidal Stability of Neutral Amphiphilic Polymers in Water. In Conformation-Dependent Design of Sequences in Copolymers II; Springer-Verlag: Berlin/Heidelberg; pp 1–85.

(160) Molnar, A.; Lakat, T.; Hosszu, A.; Szebeni, B.; Balogh, A.; Orfi, L.; Szabo, A. J.; Fekete, A.; Hodrea, J. Lyophilization and Homogenization of Biological Samples Improves Reproducibility and Reduces Standard Deviation in Molecular Biology Techniques. Amino Acids 2021, 53 (6), 917–928.

(161) Sarkar, S.; Mondal, J. Mechanistic Insights on ATP's Role as a Hydrotrope. J Phys Chem B 2021, 125 (28), 7717–7731.

(162) Heyda, J.; Okur, H. I.; Hladílková, J.; Rembert, K. B.; Hunn, W.; Yang, T.; Dzubiella, J.; Jungwirth, P.; Cremer, P. S. Guanidinium Can Both Cause and Prevent the Hydrophobic Collapse of Biomacromolecules. J Am Chem Soc 2017, 139 (2), 863–870.

(163) Hill, T. L. An Introduction to Statistical Thermodynamics; Dover Publications: New York, 1986.

(164) Bellissent-Funel, M.-C.; Hassanali, A.; Havenith, M.; Henchman, R.; Pohl, P.; Sterpone, F.; van der Spoel, D.; Xu, Y.; Garcia, A. E. Water Determines the Structure and Dynamics of Proteins. Chem Rev 2016, 116 (13), 7673–7697.

(165) Duboué-Dijon, E.; Fogarty, A. C.; Hynes, J. T.; Laage, D. Dynamical Disorder in the DNA Hydration Shell. J Am Chem Soc 2016, 138 (24), 7610–7620.

(166) Berne, B. J.; Weeks, J. D.; Zhou, R. Dewetting and Hydrophobic Interaction in Physical and Biological Systems. Annu Rev Phys Chem 2009, 60 (1), 85–103.

(167) Grossman, M.; Born, B.; Heyden, M.; Tworowski, D.; Fields, G. B.; Sagi, I.; Havenith, M. Correlated Structural Kinetics and Retarded Solvent Dynamics at the Metalloprotease Active Site. Nat Struct Mol Biol 2011, 18 (10), 1102–1108.

(168) Ball, P. Water as an Active Constituent in Cell Biology. Chem Rev 2008, 108 (1), 74–108.

(169) Aseyev, V.; Tenhu, H.; Winnik, F. M. Non-Ionic Thermoresponsive Polymers in Water; 2010; pp 29–89.

(170) Cabane, E.; Zhang, X.; Langowska, K.; Palivan, C. G.; Meier, W. Stimuli-Responsive Polymers and Their Applications in Nanomedicine. Biointerphases 2012, 7 (1).

(171) Jungwirth, P. Biological Water or Rather Water in Biology? J Phys Chem Lett 2015, 6 (13), 2449–2451.

(172) Gierszal, K. P.; Davis, J. G.; Hands, M. D.; Wilcox, D. S.; Slipchenko, L. V.; Ben-Amotz, D. π-Hydrogen Bonding in Liquid Water. J Phys Chem Lett 2011, 2 (22), 2930–2933.

(173) Perera, P.; Wyche, M.; Loethen, Y.; Ben-Amotz, D. Solute-Induced Perturbations of Solvent-Shell Molecules Observed Using Multivariate Raman Curve Resolution. J Am Chem Soc 2008, 130 (14), 4576–4577.

(174) Perera, P. N.; Fega, K. R.; Lawrence, C.; Sundstrom, E. J.; Tomlinson-Phillips, J.; Ben-Amotz, D. Observation of Water Dangling OH Bonds around Dissolved Nonpolar Groups. Proceedings of the National Academy of Sciences 2009, 106 (30), 12230–12234.

(175) Lawton, W. H.; Sylvestre, E. A. Self Modeling Curve Resolution. Technometrics 1971, 13 (3), 617.